PHYSICAL REVIEW A VOLUME 18, NUMBER 2 AUGUST 1978

Complex potential and electron spectrum in atomic collisions involving fast electronic transitions: Penning and associative ionization

Ronald James Bieniek
Department of Astronomy, University of Illinois, Urbana, Illinois 61801

(Received 25 August 1977)

Beginning with a Feshbach projection-operator analysis, formulas for the local complex potential in the entrance-channel radial wave equation are reviewed and developed in detail for inelastic atom-atom collisional processes that involve an electronic transition between Born-Oppenheimer states. Penning and associative ionization are used as illustrative examples in the presentation. A complete derivation of T-matrix elements involving radial wave functions is then presented in the context of transition rates and inelastic differential cross sections (both for energy and angle). Two approximate formulas for the energy spectrum of the particle ejected in the electronic transition are developed in which quantities obtained from exact, complex radial wave functions are replaced by those obtained from approximate, totally real radial wave functions. Numerical computations for the electron energy spectrum of the Penning process $\mathrm{He}(1s2s,2^3S)+\mathrm{H}(1s,1^2S)\rightarrow\mathrm{He}(1s^2,1^1S)+\mathrm{H}^++e^-$ are then presented to probe the effects of the imaginary width of the complex potential. It is found that the real component of the entrance-channel radial wave function is not much affected by the imaginary width when the width is small compared to other energy terms. In such cases, the imaginary component of the wave functions is then $\pi/2$ out of phase with respect to the real component, even at fairly close separations, owing to their asymptotic boundary conditions. This result also leads to a method of estimating the contribution of the imaginary radial wave functions to matrix elements using information obtained only from approximate, totally real wave functions. Finally, the eigenenergies of all 149 rotational-vibrational states of $\mathrm{HeH}^+(^1\Sigma^+)$ are reported, along with the computed cross sections of associative ionization to each state.

I. INTRODUCTION

Penning and associative ionization processes illustrate a number of characteristic features and theoretical techniques that are relevant to many other inelastic collisional processes. In their most general sense, these ionization processes involve the collision of a metastable atom or molecule (A^*) with a target atom or molecule in its ground state (B). In Penning ionization, the target is ionized when the excited species is induced to return to its ground state during the collisional encounter

$$A^*+B\rightarrow A+B^++e^-. \tag{1}$$

This process is named after one of its original investigators.[1] The related process of associative ionization produces a charged molecule:

$$A^*+B\rightarrow AB^++e^-. \tag{2}$$

These ionization processes are of practical interest because of their importance in planetary atmospheres and lasers.[2,3]

In Sec. II of this paper, we will review and develop a formalism to describe the T matrix for these processes using Feshbach projection operators. In Sec. III, we will derive a local approximation to the complex potential that arises in the radial wave equation of the entrance channel owing to the inelastic nature of the collision. In Sec. IV, we will develop various formulas for the angular- and energy-differential cross sections of the electrons ejected in the electronic transition. These same formulas are also applicable to numerous other collisional processes in which the nuclei move on well-defined Born-Oppenheimer intermolecular potentials after an electronic transition that emits (or absorbs) an electron or photon. In Sec. V of this paper, we will numerically examine the Penning and associative ionization processes involving metastable helium and atomic hydrogen:

$$\mathrm{He}(1s2s,2\,^3S)+\mathrm{H}(1s,1\,^2S)\rightarrow\mathrm{He}(1s^2,1\,^1S)+\mathrm{H}^++e^-, \tag{3}$$

$$\mathrm{He}(1s2s,2^3S)+\mathrm{H}(1s,1\,^2S)\rightarrow\mathrm{HeH}^+(^1\Sigma^+)+e^-. \tag{4}$$

This particular system was chosen because of the relative abundance of theoretical and experimental information available on it. The main thrust of these computations was to use the formulas developed in Secs. III and IV to analyze the effects that the complex potential has on these processes. Specifically, we will examine how the T-matrix elements are modified by the presence of the imaginary component of the complex potential in the equation for the radial wave function of the entrance channel. Formulas similar to those developed in Secs. II–IV have appeared elsewhere in the literature, chiefly in the work of Nakamura.

However, in his main paper on Penning ionization, Nakamura's result implicitly assumed that the electronic transition amplitude was spherically symmetric, which is not correct.[4] However, in a later paper on associative ionization, he did report a more general formula.[5] In a second paper on associative ionization, Koike and Nakamura presented a formula for the T-matrix elements relevant to these processes.[6] However, their formula differs from the one that will be developed in this paper, owing mainly, apparently, to an error in choosing the formal asymptotic condition of the product wave functions. The problems that do exist with the formulas found in the literature are due to missteps in the detailed derivation of them and/or from a lack of clarity in terms, definitions, or premises. Since only the bare framework of derivations has appeared in the literature, this author felt it would be worthwhile if a more complete presentation would appear. This is the major purpose of Secs. II–IV. In addition, when approximations are introduced, they will be explicitly identified and their physical basis discussed. It is hoped that this more complete and consolidated treatment will prove useful and informative to both beginning and experienced investigators of this and related processes.

II. GENERAL FORMALISM

The initial development of quantum-mechanical formalisms to deal with Penning and associative ionization processes is chiefly found in the work of Mori.[7-9] These processes occur because the quasimolecule formed by the colliding species may have a bound, metastable electronic configuration or an ionized continuum configuration. In essence, the bound metastable state is embedded in a continuum of ionized states. Mori and Nakamura derived expressions for the complex potential of the entrance channel using Fano's treatment of the interaction of a discrete state with a continuum of states in which it is embedded.[4,10-14]

In this section, we will employ the Feshbach projection-operator technique to obtain the basic equations for the complex potential and T-matrix elements.[15,16] The derivation follows the treatment of dissociative attachment presented by O'Malley, and reviewed by Bottcher.[17,18] We will use the following notation. A double bra, $\langle\langle\Psi|$, or ket, $|\Psi\rangle\rangle$, will denote states that include a complete nuclear and electronic configuration. A single bra, $\langle\psi|$, or ket, $|\phi\rangle$, will be used for states that are either nuclear or electronic, but not both.

Let $|\phi_d\rangle = |\phi_{A^*B}\rangle$ be the discrete Born-Oppenheimer electronic state embedded in the continuum. It is constructed from asymptotically decaying orbitals. They are combined in a way that stabilizes $\langle\phi_d|H_{el}|\phi_d\rangle$ as a local minimum in energy.[19] It is normalized such that $\langle\phi_d|\phi_d\rangle = 1$. Continuum states, which are characterized by an ejected electron with energy ε and direction $\hat{\omega}$, are denoted by $|\phi_{\vec{\varepsilon}}\rangle = |\phi_{AB^+}, e^-(\varepsilon, \hat{\omega})\rangle$. $|\phi_{AB^+}\rangle$ is the Born-Oppenheimer electronic state of the ionized molecular core, and $\vec{\varepsilon} = \epsilon\hat{\omega}$. $\hat{\omega}$ is the unit vector in the asymptotic direction of the free electron. These states have a density of $\rho(\vec{\varepsilon})$. The projection operators associated with these states are

$$Q = |\phi_d\rangle\langle\phi_d| \tag{5a}$$

and

$$P = \int d\vec{\varepsilon}\, |\phi_{\vec{\varepsilon}}\rangle\rho(\vec{\varepsilon})\langle\phi_{\vec{\varepsilon}}| \tag{5b}$$

which project onto the metastable and continuum states, respectively. A significant, but reasonable, assumption that will now be made is that all other electronic channels can be neglected during a collision. For example, photon decay back to the ground neutral state will not be included. The excited state is called metastable for the very reason that the transition amplitude to such states is very small. At thermal energies, the coupling to other excited channels is weak owing to the energy separation between them. Stated differently, this says that the metastable plus the continuum states adequately approximated a complete set; i.e., $P+Q \simeq 1$, from the manner in which $|\phi_d\rangle$ is constructed. Note that this also implies that $P^2 = P$, $Q^2 = Q$, and $PQ = QP = 0$.

We now write the time-independent Schrödinger equation for the system:

$$(H-E)|\Psi\rangle\rangle = 0. \tag{6}$$

By using $P+Q=1$, we can obtain

$$(H_{PP}-E)P|\Psi\rangle\rangle = -H_{PQ}|\Psi\rangle\rangle \tag{7a}$$

and

$$(H_{QQ}-E)Q|\Psi\rangle\rangle = -H_{QP}|\Psi\rangle\rangle\,, \tag{7b}$$

where

$$H_{PP} = PHP \quad\text{and}\quad H_{PQ} = PHQ. \tag{7c}$$

It is now convenient to introduce states that approximate the complete metastable and continuum states. These are the solutions of the uncoupled homogeneous equations

$$(H_{QQ}-E)Q|\Psi_Q\rangle\rangle = 0 \tag{8a}$$

and

$$(H_{PP} - E)P|\Psi_P\rangle\rangle = 0. \tag{8b}$$

By applying the state $\langle\phi_d|$ onto Eq. (8a) from the left-hand side, it becomes

$$(T_N + V_d - E)|\psi_d\rangle = 0\,, \tag{9}$$

where $V_d = \langle\phi_d|H_{el}|\phi_d\rangle$ and $|\psi_d\rangle = \langle\phi_d|\Psi_Q\rangle\rangle$. To obtain this, we have made the standard Born-Oppenheimer approximation that the nuclear kinetic operator has a negligible effect on the electronic states; e.g., $\langle\phi_d|T_N|\phi_d\rangle \simeq 0$. This is equivalent to the position-space coordinate equation

$$[T_N(\vec{R}) + V_d(\vec{R}) - E]\psi_d(\vec{R}) = 0\,, \tag{10}$$

where $T_N(\vec{R})$ is the kinetic energy term, $V_d(\vec{R})$ is the unperturbed intermolecular potential of the metastable state, and $\psi_d(\vec{R})$ is the wave function of the nuclei. $\vec{R} = R\hat{R}$ is the position vector of the internuclear separation.

The T matrix for transitions to an ionized final state is[16]

$$T = \langle\langle\Psi_p^-|PHQ|\Psi^+\rangle\rangle = \langle\langle\Psi_p^-|PH|\phi_d\rangle\langle\phi_d|\Psi^+\rangle\rangle. \tag{11}$$

$|\Psi^+\rangle\rangle$ is the complete state of the total system, while $|\Psi_p^-\rangle\rangle$ represents only the ionized states. The "+" and "−" superscripts refer, respectively, to boundary conditions of asymptotically outgoing and incoming scattered waves. In the operator PHQ, Q selects the metastable state, H operates on it, and P selects the ionized states that result from this operation. The object of this projection-operator analysis is to produce an equation for

$$|\chi_d^+\rangle = \langle\phi_d|\Psi^+\rangle\rangle\,, \tag{12}$$

so that the T matrix becomes

$$T = \langle\langle\Psi_p^-|PH|\phi_d\rangle|\chi_d^+\rangle\,. \tag{13}$$

In this form, it is apparent that the total state wave function has been separated into an electronic state $|\phi_d\rangle$ and a state $|\chi_d\rangle$ of effective nuclear motion.

To obtain an equation for $|\chi_d^+\rangle$, we consider the quantity $Q|\Psi^+\rangle\rangle$. Equation (7b) is the inhomogeneous equation for $Q|\Psi^+\rangle\rangle$. The solution of this equation is, therefore, the sum of the homogeneous solution [cf. Eq. (8a)], and a particular solution that satisfies the boundary conditions. Thus $Q|\Psi^+\rangle\rangle$ can formally be written

$$Q|\Psi^+\rangle\rangle = Q|\Psi_Q^+\rangle\rangle + G_Q^+ QHP|\Psi^+\rangle\rangle\,, \tag{14a}$$

where

$$G_Q^+ = [Q(E + i\epsilon - H)Q]^{-1} \tag{14b}$$

and ϵ is a vanishing small positive number. The physical interpretation of this is that $Q|\Psi^+\rangle\rangle$ is composed of an incident wave describing the nuclear motion in the metastable state, represented by $Q|\Psi_Q^+\rangle\rangle$, and a scattered wave of the ionized state, represented by $G_Q^+ QHP|\Psi^+\rangle\rangle$. Since the initial channel has no ionized-state component, the coefficient of the homogeneous solution $P|\Psi_P^+\rangle\rangle$ is zero in the analogous equation for $P|\Psi^+\rangle\rangle$:

$$P|\Psi^+\rangle\rangle = G_P^+ PHQ|\Psi^+\rangle\rangle. \tag{15}$$

Substituting this into Eq. (14) and rearranging, we have

$$Q|\Psi^+\rangle\rangle = (1 - G_Q^+ QHPG_P^+ PHQ)^{-1} Q|\Psi_Q^+\rangle\rangle. \tag{16}$$

Using this, the T matrix is

$$T = \langle\langle\Psi_P^-|PH|\phi_d\rangle A\langle\phi_d|\Psi_Q^+\rangle\rangle\,, \tag{17a}$$

where

$$A = |1 - g_d^+ F^+|^{-1} \tag{17b}$$

with

$$g_d^+ = \langle\phi_d|G_Q^+|\phi_d\rangle = (E + i\epsilon - T_N - V_d)^{-1}\,, \tag{17c}$$

$$F^+ = \langle\phi_d|HPG_P^+PH|\phi_d\rangle. \tag{17d}$$

By comparing Eq. (13) with Eq. (17), we see that

$$|\chi_d^+\rangle = A|\psi_d^+\rangle\,. \tag{18}$$

These states should actually have energy and direction labels to indicate the boundary conditions of total energy and asymptotic direction; e.g., $|\psi_d^+(\vec{E})\rangle$ and $|\psi_d^+(\vec{E})\rangle$, where $\vec{E} = E\hat{\Omega}$. E is the magnitude of the total energy of the channel and $\hat{\Omega}$ is a unit vector in the asymptotic direction of the unscattered component of the wave function. These labels will be suppressed unless they are needed to clarify a particular point.

Using Eqs. (9) and (18), we find that $|\chi_d^+\rangle$ is the solution of

$$(T_N + V_d + F^+ - E)|\chi_d^+\rangle = 0. \tag{19}$$

This is now in a form that can usefully be put into coordinate-space notation by applying $\langle\vec{R}|$ on the left-hand side and inserting

$$1 = \int d\vec{R}'\,|\vec{R}'\rangle\langle\vec{R}'|\,;$$

we obtain

$$[T_N(\vec{R})+V_d(\vec{R})-E]\chi_d^+(\vec{R}) = -\int d\vec{R}'\langle\vec{R}|F^+|\vec{R}'\rangle\chi_d^+(\vec{R}'). \quad (20)$$

Using the fact that the continuum electronic states form a complete set,

$$1=\int d\vec{\varepsilon}\;|\phi_{\vec{\varepsilon}}\rangle\rho(\vec{\varepsilon})\langle\phi_{\vec{\varepsilon}}|\;,$$

we can rewrite the operator term in the F^+ term as

$$\begin{aligned}\langle\vec{R}|F^+|\vec{R}'\rangle &= \langle\vec{R}|\langle\phi_d|H\int d\vec{\varepsilon}\,d\vec{\varepsilon}'\;|\phi_{\vec{\varepsilon}}^+\rangle\rho(\vec{\varepsilon})\langle\phi_{\vec{\varepsilon}}^+|G_P^+|\phi_{\vec{\varepsilon}'}^+\rangle \\ &\qquad\times\rho(\vec{\varepsilon})\langle\phi_{\vec{\varepsilon}'}^+|H|\phi_d\rangle|\vec{R}'\rangle \\ &=\langle\vec{R}|\langle\phi_d|H|\int d\vec{\varepsilon}\,|\phi_{\vec{\varepsilon}}^+\rangle g_c^+\langle\phi_{\vec{\varepsilon}}^+|H|\phi_d\rangle|\vec{R}'\rangle \\ &= d\vec{\varepsilon}\,\langle\vec{R}|\vec{\varepsilon}^+\rangle\langle\vec{R}|g_c^+|\vec{R}'\rangle\langle\vec{\varepsilon}^+|\vec{R}'\rangle\,, \end{aligned} \quad (21a)$$

where

$$\langle\vec{\varepsilon}^{\pm}|\vec{R}'\rangle=\int d\vec{R}\,\langle\vec{R}|\langle\phi_{\vec{\varepsilon}}^{\pm}H_{\text{el}}|\phi_d\rangle|\vec{R}'\rangle \quad (21b)$$

and

$$g_c^+=\lim_{\epsilon\to 0}(E+i\epsilon-\varepsilon-T_N-V_c)^{-1}. \quad (21c)$$

V_c is the intermolecular-potential operator arising from the ionized-continuum electronic state. This explicitly assumes that the Born-Oppenheimer terms, $\langle\phi_{\vec{\varepsilon}}|T_N|\phi_d\rangle$, can be neglected and set equal to zero. As it turns out, $\langle\vec{\varepsilon}|\vec{R}\rangle$ is the transition amplitude for autoionization at the internuclear separation $\vec{R}$. The space-coordinate representation of $\langle\vec{\varepsilon}|\vec{R}\rangle$ is

$$\langle\vec{\varepsilon}^{\pm}|\vec{R}\rangle=\int d\vec{r}_N\,\phi_{\vec{\varepsilon}}^{\pm}(\vec{r}_N|\vec{R})^*H_{\text{el}}\,\phi_d(\vec{r}_N|\vec{R}), \quad (22)$$

where $\{\vec{r}_N\}$ is the set of position vectors of the electrons.

To proceed, we must remove the operator g_c^+, which contains V_c. This can be accomplished by making a spectral decomposition using a complete set of nuclear wave-function states in the ionized channel. These are solutions of the equation

$$(g_c^+)^{-1}|\psi_P^+(\vec{E}')\rangle\rangle=(E'-T_N-V_c)|\psi_P^+(\vec{E}')\rangle\rangle=0. \quad (23)$$

Using this as a basis set, the unity operator is

$$1=\int d\vec{E}'\;|\psi_P^+(\vec{E}')\rangle\rangle\rho(\vec{E}')\langle\psi_P^+(\vec{E}')|\,.$$

$\rho(\vec{E}')$ is the density of states per unit energy per unit solid angle. For associative ionization ($E'<0$), $\rho(\vec{E}')=(4\pi)^{-1}\delta(E-E_{v'}^{J'})$ where v' stands for the vibrational level of the molecular ion AB^+, and J' is its rotational quantum number with projection M'. The factor of $(4\pi)^{-1}$ in $\rho(\vec{E}')$ for $E'<0$ is introduced to nullify the effects of the integral over $\hat{\Omega}'$ for bound states, since such integration has no meaning for associative ionization. However, by employing this "trick," we simplify the derivation since we can then formally use the same formulas for both Penning and associative ionization. This poses no real problem because the angular density of states can be resolved into angular and magnitude components; i.e., $\rho(\vec{E})=\rho(E)\rho(\hat{\Omega})$. In this specific case, the unity operator is

$$\begin{aligned}1&=\int_0^\infty d\vec{E}'\;|\psi_P^+(\vec{E}')\rangle\rangle\,\rho(\vec{E}')\langle\psi_P^+(\vec{E}')| \\ &\quad+\sum_{J'}\sum_{M'}\sum_{v'}|\psi_P^{M'}(E_{v'}^{J'})\rangle\rangle\langle\psi_P^{M'}(E_{v'}^{J'})| \\ &=\int d\vec{E}'\;|\psi_P^+(\vec{E}')\rangle\rangle\rho(\vec{E}')\langle\psi_P^+(\vec{E}')|\,.\end{aligned}$$

Substituting Eq. (23) into $\langle\vec{R}|g_c^+|\vec{R}'\rangle$ yields

$$\begin{aligned}\langle\vec{R}|g_c^+|\vec{R}'\rangle&=\lim_{\epsilon\to 0}\langle\vec{R}|1(E+i\epsilon-\varepsilon-T_N-V_c)^{-1}1|\vec{R}'\rangle \\ &=\lim_{\epsilon\to 0}\int d\vec{E}'\frac{\langle\vec{R}|\psi_P^+\rangle\rho(\vec{E}')\langle\psi_P^+|\vec{R}'\rangle}{E+i\epsilon-\varepsilon-E'} \\ &=\int d\hat{\Omega}'\,\mathcal{P}\int dE'\,\frac{\psi_P^+(\vec{E}',\vec{R})\psi_P^+(\vec{E}',\vec{R}')^*\rho(\vec{E}')}{E-\varepsilon-E'} \\ &\quad-i\pi\int d\hat{\Omega}'\,\psi_P^+(\vec{E}_0',\vec{R})\psi_P^+(\vec{E}_0',\vec{R}')^*\rho(\vec{E}_0'),\end{aligned} \quad (24)$$

where $E_0'=E-\varepsilon$ (energy-conserving states) and $\mathcal{P}\int$ denotes the principal value of the integral. With this, the goal has been achieved to find the equation for the effective nuclear wave function $\chi_d^+(\vec{E},\vec{R})$. Substituting Eq. (24) into Eq. (21), and this into Eq. (20), we finally have the equation for $|\chi_d^+(\vec{E},\vec{R})\rangle$:

$$\begin{aligned}[T_N(\vec{R})+V_d(\vec{R})-E]\chi_d^+(\vec{E},\vec{R}) &=+i\pi\int d\vec{\varepsilon}\,d\hat{\Omega}'\,d\vec{R}'\,K(\vec{\varepsilon},\vec{E}_0',\vec{R},\vec{R}')\chi_d^+(\vec{E},\vec{R}') \\ &\quad-\int d\vec{\varepsilon}\,d\hat{\Omega}'\,\mathcal{P}\int dE'\,dR'\,\frac{K(\vec{\varepsilon},\vec{E}',\vec{R},\vec{R}')}{E-\varepsilon-E'}\chi_d^+(\vec{E},\vec{R}'),\end{aligned} \quad (25a)$$

where

$$K(\vec{\varepsilon},\vec{E}',\vec{R},\vec{R}')=\rho(\vec{\varepsilon})\rho(\vec{E}')\langle\vec{\varepsilon}^+|\vec{R}\rangle^*\langle\vec{\varepsilon}^+|\vec{R}'\rangle \times\psi_P^+(\vec{E}',\vec{R})\psi_P^+(\vec{E}',\vec{R}')^*\,. \quad (25b)$$

III. RADIAL EQUATIONS

In scattering calculations, the standard procedure is to construct the scattered wave functions from partial waves composed of the product of angular and radial eigenfunctions. For spherically symmetric potentials, the problem of determining a wave function is reduced to solving a second-order differential equation for the radial eigenfunction. By decomposing the complex initial-channel wave function into partial waves, we can bring standard numerical techniques to bear on the solution of Eq. (25).

We begin by making the partial-wave expansion for the initial wave function[20]

$$\chi_d^+(\vec{\mathrm{E}},\vec{\mathrm{R}})=\sum_{JM}Y^*_{JM}(\hat{\Omega})Y_{JM}(\hat{R})(i)^J \times\exp(i\bar{\eta}_i^J)\bar{F}_i^J(E,R)R^{-1}\,. \tag{26}$$

In elastic processes, the conservation of channel flux demands that the phase shift, η_i^J, is real. However, in inelastic scattering, where transitions to other channels occur, flux is lost from the initial channel. Thus, the phase shift is, in general, complex.[21] The bar over $\bar{\eta}_i^J$ is used to indicate this. The bar over $\bar{F}_i^J(E,R)$ signifies the radial wave function is then also complex.

A similar expansion can also be made for the final-state nuclear-continuum wave function resulting from Penning ionization:

$$\psi_p^\pm(\vec{\mathrm{E}}',\vec{\mathrm{R}})=\sum_{J'M'}Y^*_{J'M'}(\hat{\Omega}')Y_{J'M'}(\hat{R})(i)^{J'} \times\exp(\pm i\eta_f^{J'})F_f^{J'}(E',R)R^{-1}. \tag{27}$$

The expansion for $\psi_p^-(\vec{\mathrm{E}},\vec{\mathrm{R}})$ has been obtained from the reciprocity relationship $\psi_p^-(E,\hat{\Omega},\vec{\mathrm{R}})=\psi_p^+(E,-\hat{\Omega},\vec{\mathrm{R}})^*$.[22] Since there are no electronic transitions out of the final state within the Born-Oppenheimer approximation, the nuclear phase shifts and radial wave functions are real. To indicate $F_f^{J'}$ is totally real, no bar is put above it. In the case of associative ionization, the atoms are bound in a molecule. For a discrete final state, the wave function is simply

$$\psi_p^{M'}(E_{v'}^{J'},\vec{\mathrm{R}})=Y_{J'M'}(\hat{R})F_f^{J'}(E_{v'}^{J'},R)R^{-1}. \tag{28}$$

Equation (23) is the wave equation for the final states. The potentials considered here are spherically symmetric; we can explicitly denote this by expressing these as

$$V_i(R)=V_d(\vec{\mathrm{R}}) \tag{29a}$$

and

$$V_f(R)=V_c(\vec{\mathrm{R}})\,, \tag{29b}$$

where the subscripts i and f refer to initial and final states. The final-state wave equation can then be simplified. By inserting the final-state partial-wave expansion [Eq. (27)] into Eq. (23), multiplying by $Y_{J'M'}(\hat{\Omega}')Y^*_{J'M'}(\hat{R})$, integrating over $\hat{\Omega}'$ and $\hat{R}$, and using the orthonormality properties of the spherical harmonics [Eq. (B5a)], the final-state radial wave equation is

$$\left(-\frac{\hbar^2}{2\mu}\frac{d^2}{dR^2}+V_f(R)+\frac{\hbar^2}{2\mu}\frac{J'(J'+1)}{R^2}-E'\right)F_f^{J'}(E',R)=0, \tag{30a}$$

where asymptotically

$$F_s^J(E,R)\sim A(E,\mu)\sin(kR-\tfrac{1}{2}J\pi+\eta_s^J)\,. \tag{30b}$$

$\mu=m_1m_2/(m_1+m_2)$ is the reduced mass of the nuclei and $A(E,\mu)$ is a normalization constant For associative ionization, we multiply Eq. (28) by $Y^*_{J'M'}(\hat{R})$ and integrate over $\hat{R}$ to obtain Eq. (30a) again. However, instead of having Eq. (30b) as an asymptotic condition, the bound molecular wave function decays exponentially.

Before we can produce a radial equation for the initial state, we have to make a spherical harmonic expansion of the electronic wave functions in the transition amplitude $\langle\vec{\varepsilon}\,|\vec{\mathrm{R}}\rangle$. To see how this is done, we must turn to the manner in which the electronic wave functions are constructed. Physically, the electronic transition is a molecular autoionization from a metastable to continuum electronic configurations. One approach is to construct wave functions through a configuration-interaction (CI) calculation and choose the eigenstate and energy that approach the right limits when the nuclei are asymptotically separated.[19]

Miller *et al.* have used this method in their electronic calculations for the Penning process involving metastable helium and atomic hydrogen.[23] In their approach, the metastable wave function $|\phi_d\rangle$ was an N-electron CI wave function constructed from Slater determinants whose elements are obtained from a chosen set of molecular orbitals. The continuum state $|\phi_{\vec{\varepsilon}}\rangle$ is another N-electron CI wave function whose Slater determinants are composed of $N-1$ bound orbitals taken from the same set used for the metastable state. These represent the ionic part of the configuration. The Nth orbital, however, is a continuum. This orbital is constructed from a partial-wave expansion

$$\phi^\pm(\vec{\varepsilon},\vec{\mathrm{r}}\,|\vec{\mathrm{R}})=\sum_l Y^*_{lm}(\hat{\omega})_{\hat{R}}Y_{lm}(\hat{r})_{\hat{\mathrm{R}}}(i)^l \times\exp(\pm i\sigma^l)f^l(\varepsilon,r)r^{-1}, \tag{31a}$$

where the radial wave function behaves asymptotically as a Coulomb wave function:

$$f^l(\varepsilon,r)\sim a(\varepsilon,m_e)\sin[kr+k^{-1}\ln(2kr)-\tfrac{1}{2}l\pi+\sigma^l]\,, \tag{31b}$$

where $k=(2m_e\varepsilon/\hbar^2)^{1/2}$ and $a(\varepsilon,m_e)$ is the normalization factor. The angular arguments of the spherical harmonics, $(\hat{\omega})_{\hat{R}}$ and $(\hat{r})_{\hat{R}}$, indicate that the solid angles related to electronic vectors ($\hat{\omega}$ and $\hat{r}$) are to be measured in a coordinate system whose z axis lies along the direction of the internuclear axis $\hat{R}$. The continuum orbital is centered on the target nuclei B because of the electron-exchange nature of the process.[24,25] There is no sum over the magnetic quantum number m because the projection of the total electronic angular momentum is conserved within the Born-Oppenheimer approximation. Thus we have $m=\Lambda_*-\Lambda_{\text{ion}}$, where the Λ are the usual quantum numbers of the projection of the total electronic angular momentum associated with the bound metastable and ionic states.[26]

By substituting Eq. (31) into Eq. (22), we have

$$\langle\vec{\varepsilon}^{\pm}|\vec{R}\rangle=\sum_l Y_{lm}(\hat{\omega})_{\hat{R}}(-i)^l\exp(\mp i\sigma_l)\langle\phi_{\varepsilon lm}|H-E\,|\,\phi_d\rangle\,, \tag{32}$$

where $\phi_{\varepsilon lm}$ represents the position-space part of total final-state electronic wave function containing $Y_{lm}(\hat{r})_{\hat{R}}f^l(\varepsilon,r)$. The last factor is an integral over the position space of the N electrons. For convenience we define

$$\langle\varepsilon^{\pm}lm\,|R\rangle=(-i)^l\exp(\mp i\sigma^l)\langle\phi_{\varepsilon lm}|H-E\,|\,\phi_d\rangle \tag{33}$$

for future use. The parametric dependence of the electronic wave functions and coupling element on the internuclear separation R is explicitly indicated.

To evaluate the effect of the electronic coupling element on nuclear motion and differential cross sections, we refer all angles to the center-of-mass (c.m.) coordinate system of the colliding nuclei and not their internuclear axis. To do this, we will employ rotation operators using the conventions found in Edmonds.[27] $\hat{\omega}$ is the direction of the ejected electron and $\hat{R}$ is the direction of the internuclear axis in the c.m. coordinate system. To go from the internuclear-axis coordinate system of the electrons to the c.m. system of the nuclei, we must rotate the coordinate axes by $\hat{R}^{-1}$, the inverse of $\hat{R}$. The relationship between the angular momentum eigenfunctions in the new and old system is [Eq. (4.14) in Edmonds]

$$Y_{lm}(\hat{\omega})_{\hat{R}}=\sum_k Y_{lk}(\hat{\omega})D^l_{km}(\alpha\beta\gamma)\,, \tag{34}$$

where D^l_{km} is a rotation matrix whose arguments, $(\alpha\beta\gamma)$, are the Euler angles associated with the rotation $\hat{R}^{-1}$. By looking at the diagram of the Euler angles in Fig. 1, we find $\hat{R}=(\hat{R}^{-1})^{-1}=(\alpha\beta\gamma)^{-1}=(\pi-\gamma,\beta,\pi-\alpha)$. This choice is necessary to keep all angles between 0 and 2π. Using the definition of the rotation matrices, we have [Eq. (B1a)]

$$\begin{aligned}D^l_{km}(\hat{R}^{-1})&=e^{ik\alpha}d^l_{km}(\beta)e^{im\gamma}\\&=[e^{im(\pi-\gamma)}d^l_{mk}(\beta)e^{ik(\pi-\alpha)}]^*\\&=D^l_{mk}(\hat{R})^*=(-1)^{m-k}D^l_{-m-k}(\hat{R})\,.\end{aligned} \tag{35}$$

[The $d^l_{mk}(\beta)$ are discussed in Edmonds.] Now let $\alpha'=\pi-\gamma$, $\beta'=\beta$, and $\gamma'=\pi-\alpha$. The angles $(\alpha'\beta'\gamma')$ refer to the order of rotations about the new axes produced by the previous rotation; i.e., $D(\alpha'\beta'\gamma')=D_{z''}(\gamma')D_{y'}(\beta')D_z(\alpha')$, where the primed axes represent the new coordinate system following each rotation. In this convention, vectors remain stationary in space, while the coordinate system is rotated. However, we want the c.m. frame to remain fixed while vectors are moved. Consequently, the angles (θ,ϕ) that represent the position vector $\hat{R}$ in the c.m. frame are associated with the last two rotations in Edmonds' convention. Thus the Euler angles are related to the normal spherical coordinates of $R=(\theta,\phi)$ by $\alpha'=0$, $\beta'=\theta$, and $\gamma'=\phi$. With this understanding and use of Eq. (B1b), the electronic coupling element [Eq. (32)] becomes

$$\langle\vec{\varepsilon}^{\pm}|\vec{R}\rangle=\sum_{lk}Y^*_{lk}(\hat{\omega})(-1)^m D^l_{-mk}(\hat{R})\langle\varepsilon^{\pm}lm|R\rangle\,. \tag{36}$$

Using Eqs. (26), (27), and (36), we can simplify the form of the complex nonlocal integral of the initial channel [Eq. (25)] to produce a radial equation that is much simpler to solve numerically. By writing the left-hand side of Eq. (25) in spheri-

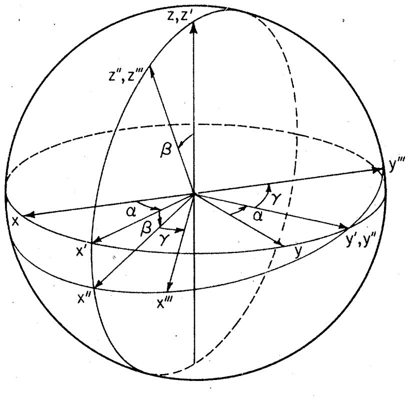

FIG. 1. Euler angles associated with the rotations of coordinate axes. [Adapted from A. R. Edmonds, *Angular Momentum in Quantum Mechanics* (Princeton U.P., Princeton, N. J., 1960).]

cal coordinates and then substituting in the partial-wave expansion for the nuclear wave function [Eq. (26)], the Schrödinger equation for the initial channel becomes

$$\sum_{JM} Y^{*}_{JM}(\hat{\Omega})Y_{JM}(\hat{R})(i)^{J}\exp(i\bar{\eta}^{J}_{i})\left(\frac{2J+1}{4\pi}\right)^{1/2}R^{-1}$$

$$\times\left(-\frac{\hbar^2}{2\mu}\frac{d^2}{dR^2}+V_i(R)+\frac{\hbar^2}{2\mu}\frac{J(J+1)}{R^2}-E\right)$$

$$\times\bar{F}^{J}_{i}(E,R)=I_{\mathrm{CN}}, \qquad (37)$$

where I_{CN} stands for the complex nonlocal integral on the right-hand side of Eq. (25). The imaginary part of I_{CN} is the formal means of representing absorption of flux out of the entrance channel. The real part represents the level shift caused by coupling to the continuum channels. Together, they produce the effective optical potential of the initial channel. The imaginary part of I_{CN} will be considered in detail. The real part follows from a similar analysis.

By substituting the partial-wave expansions of Eqs. (26), (27), and (36) into the left-hand side of Eq. (25), the contribution of Penning ionization to the imaginary part of I_{CN} becomes

$$\mathrm{Im}(I_{\mathrm{CN}})=\pi\int d\hat{\Omega}'\,d\varepsilon\,d\hat{\omega}\,R'^2\,dR'\,d\hat{R}'\sum_{lk}(-1)^m Y_{lk}(\hat{\omega})D^{l}_{-mk}(\hat{R})^{*}\langle\varepsilon^{+}lm\,|R\rangle^{*}$$

$$\times\sum_{uv}(-1)^m Y^{*}_{uv}(\hat{\omega})D^{u}_{-mv}(\hat{R}')\langle\varepsilon^{+}um\,|R'\rangle\,\rho(\vec{\varepsilon})$$

$$\times\sum_{J'M'}Y^{*}_{J'M'}(\hat{\Omega}')Y_{J'M'}(\hat{R})(i)^{J'}\exp(i\eta^{J'}_{f})F^{J}_{f}(E'_0,R)R^{-1}$$

$$\times\sum_{L'N'}Y_{L'N'}(\hat{\Omega}')Y^{*}_{L'N'}(\hat{R}')(-i)^{L'}\exp(-i\eta^{L'}_{f})F^{L'}_{f}(E'_0,R')(R')^{-1}$$

$$\times\sum_{JM}Y^{*}_{JM}(\hat{\Omega})Y_{JM}(\hat{R}')(i)^{J}\exp(i\bar{\eta}^{J}_{i})\bar{F}^{J}_{i}(E,R')\rho(\vec{\mathrm{E}}'_0). \qquad (38)$$

In the contribution from associative ionization, the sums over primed indices do not appear, nor do the factors involving $\hat{\Omega}'$, η_f, or $(i)^{J'}$ and $(i)^{L'}$. In the analysis that follows, we will explicitly use the asymptotically free nuclear state of Penning ionization [Eq. (27)] for the final-state wave function. The derivation for associative ionization can be obtained by simply ignoring factors of this type in what follows.

Since we must now do an integral over angles, it is necessary to discuss the normalization of quantum-mechanical states and their density. For convenience, we will employ energy-normalized wave functions. For asymptotically free states, ($\varepsilon>0$ and $E>0$), we have $\langle\phi_{\vec{\varepsilon}}|\phi_{\vec{\varepsilon}'}\rangle=\delta(\vec{\varepsilon}-\vec{\varepsilon}')$ and $\langle\psi(\vec{\mathrm{E}})|\psi(\vec{\mathrm{E}}')\rangle=\delta(\vec{\mathrm{E}}-\vec{\mathrm{E}}')$. This implies that the density of such states is unity: $\rho(\vec{\varepsilon})=\rho(\vec{\mathrm{E}})=1$ (see Appendix A). Since the angular component of the asymptotic energy parameter is independent of its magnitude, we can divide the density of states into a product, $\rho(\vec{\mathrm{E}})=\rho(E)\rho(\hat{\Omega})$. Each factor can have unit density: $\rho(E)=\rho(\hat{\Omega})=1$ for $E>0$. In this case the normalization constant is $A(E,\mu)=[2\mu/\pi\hbar^2k)]^{1/2}$, where $k=(2\mu E/\hbar^2)^{1/2}$. The bound states of associative ionization are normalized so that

$$\langle\psi^{M}_{P}(E^{J}_{v})\,|\,\psi^{M'}_{P}(E^{J'}_{v'})\rangle=\delta_K(M-M')\delta_K(J-J')\delta_K(v-v'),$$

where $\delta_K(n-m)=1$ if $n-m=0$, and is zero otherwise. This demands that

$$\int F^{L'}_{f}(E^{L'}_{u'},R)F^{J'}_{f}(E^{J'}_{v'},R)\,dR=\delta_K(L'-J')\delta_K(u'-v').$$

The density of such states is $\rho(E)=\delta(E-E^{J'}_{v'})$. For reasons already discussed in Sec. II, we can define $\rho(\hat{\Omega}')=(4\pi)^{-1}$ for $E'<0$. Although density factors are now specified, $\rho(\varepsilon)$ and $\rho(E')$ will continue to appear in the remainder of this paper to make the formulas readily useful to investigators employing other normalizations. Since the spherical harmonics are orthonormal, we can carry out the integration over $\hat{\omega}$ and $\hat{\Omega}'$ to obtain

$$\mathrm{Im}(I_{\mathrm{CN}})=\pi\int d\varepsilon\,dR'\,d\hat{R}'\sum_{lk}\sum_{J'M'}\sum_{JM}D^{l}_{-mk}(\hat{R})^{*}D^{l}_{-mk}(\hat{R}')Y_{J'M'}(\hat{R})Y^{*}_{J'M'}(\hat{R}')Y^{*}_{JM}(\hat{\Omega})Y_{JM}(\hat{R}')K(JJ'lm\,|R,R'), \qquad (39a)$$

where

$$K(JJ'lm\,|R,R') = \langle \varepsilon^+ lm\,|R\rangle^* \rho(\varepsilon) \langle \varepsilon^+ lm\,|R'\rangle \times F_f^{J'}(E_0',R) F_f^{J'}(E_0',R) \rho(E_0') \times (i)^J \exp(i\bar{\eta}_i^J) \bar{F}_i^J(E,R') R^{-1}\,. \tag{39b}$$

[For $E_0'<0$ (associative ionization), the δ function in $\rho(E_0')$ will produce the indicated sum over (J',M') when the integral over ε is made.]

To do the integral over $\hat{R}'$, we must cast the spherical harmonics into their D-matrix form [Eq. (B4b)]:

$$Y_{JM}(\hat{R}') = [(2J+1)/4\pi]^{1/2} D_{0M}^J(\alpha',\theta',\phi')$$

with $\alpha'=0$ in the present case. This reminds us that the integral over $\hat{R}'(\theta,\phi)$ is only over the Euler angles β' and γ'. The lack of the integral over α' will lead to an "unphysical" result for the general case, but a reasonable answer for a specific, but useful case often encountered.

The integral over the product of three D matrices is[27]

$$(8\pi^2)^{-1}\int_0^{2\pi} d\alpha \int_0^{\pi} \sin\beta\, d\beta \int_0^{2\pi} d\gamma\, D_{n_1m_1}^{l_1} D_{n_2m_2}^{l_2} D_{n_3m_3}^{l_3} = \begin{pmatrix} l_1 & l_2 & l_3 \\ n_1 & n_2 & n_3 \end{pmatrix} \begin{pmatrix} l_1 & l_2 & l_3 \\ m_1 & m_2 & m_3 \end{pmatrix}\,. \tag{40}$$

(The double-rowed quantities in parentheses are $3j$ symbols.) The integrals over α and γ essentially produce Kronecker δ factors in the $3j$ symbols to ensure that the sum of the n and m indices are both zero. $(2\pi)^{-1}\int d\alpha$ produces a $\delta_K(n_1+n_2+n_3)$ factor and $(2\pi)^{-1}\int d\gamma$ produces $\delta_K(m_1+m_2+m_3)$. Thus if we are only integrating over β' and γ' in Eq. (39), we have

$$\mathrm{Im}(I_{\mathrm{CN}}) = \pi \int d\varepsilon\, dR' \sum_{lk} \sum_{J'M'} \sum_{JM} D_{-mk}^l(\hat{R})^* D_{0M'}^{J'}(\hat{R}) D_{0M}^J(\hat{\Omega})^* K(JJ'lm\,|R,R')(-1)^{M'} \frac{(2J+1)(2J'+1)}{4\pi} \times \begin{pmatrix} J & J' & l \\ 0 & 0 & -m \end{pmatrix}_{\mathrm{mod}} \begin{pmatrix} J & J' & l \\ M & -M' & k \end{pmatrix}. \tag{41}$$

The subscript mod on the modified $3j$ symbol indicates it does not include the usual requirement that the lower numbers sum to zero. Explicitly, we have

$$\begin{pmatrix} J & J' & l \\ 0 & 0 & -m \end{pmatrix}_{\mathrm{mod}} \begin{pmatrix} J & J' & l \\ M & -M' & k \end{pmatrix} = \tfrac{1}{2}\delta_K(M-M'+k) \times \int \sin\beta\, d\beta\, d_{0M}^J(\beta) d_{0-M'}^{J'}(\beta) d_{-mk}^l(\beta)\,. \tag{42}$$

The lack of conservation of the projection quantum number is bothersome. The source of the problem is that we have neglected, in the derivation we have followed, the coupling of the angular momenta of the bound electronic states with that of the free particles. This is a general problem encountered in the Born-Oppenheimer approximation. More complicated treatments can be made that take this coupling into account.[28,29] However, such treatments are not within the scope or intent of this paper.

These problems can be avoided by considering only those processes in which the projection quantum numbers of the total electronic orbital angular momentum of the initial and final molecular configurations are the same; i.e., $\Lambda=\Lambda'$. In such cases, we have $m=\Lambda-\Lambda'=0$. If we use $m=0$ in the modified $3j$ symbol in Eq. (41), it becomes identical to a regular $3j$ symbol. Examples of this are the Penning and associative ionization processes given by Eqs. (3) and (4).

From this point on, we will explicitly assume that the systems under discussion have the same projection quantum numbers in the initial and final bound electronic states. By using the definition of the D matrices for $m=0$ [Eq. (B1a)], we see that

$$D_{0k}^l(\hat{R}') = (2\pi)^{-1} \int d\alpha'\, D_{0k}^l(\alpha',\beta',\gamma')\,,$$

and consequently

$$(4\pi)^{-1}\int d\hat{R}' = (8\pi^2)^{-1}\int d\alpha' \sin\beta'\, d\beta'\, d\gamma'\,.$$

Using this result, we can change the modified $3j$ symbol in Eq. (41) into a regular $3j$ symbol for the case $m=0$.

By expressing the product of two D matrices in Eq. (41) with the argument $\hat{R}$ as an expansion of single D matrices of the same argument [Eqs. (B1b) and (B2)], we can employ the orthonormality relationship of the $3j$ symbols [Eq. (B3b)], and the sum over k and M' to achieve the simplification

$$\mathrm{Im}(I_{\mathrm{CN}}) = \pi \sum_{JM} Y^{*}_{JM}(\hat{\Omega}) Y_{JM}(\hat{R}) (i)^{J} \exp(i\bar{\eta}^{J}_{i}) \sum_{J'l} (2J'+1) \begin{pmatrix} J & J' & l \\ 0 & 0 & 0 \end{pmatrix}^{2}$$

$$\times \int d\varepsilon\, dR' \langle \varepsilon^{+} l | R\rangle^{*} \langle \varepsilon^{+} l | R'\rangle \rho(\varepsilon)\; K_{f}(E'_{0}, J' | R, R') \bar{F}^{J}_{i}(E, R'), \qquad (43a)$$

where

$$K_{f}(E', J' | R, R') = F^{J'}_{f}(E', R) F^{J'}_{f}(E', R') \rho(E') \qquad (43b)$$

and

$$\langle \varepsilon^{\pm} l | R\rangle = \langle \varepsilon^{\pm} l 0 | R\rangle . \qquad (43c)$$

It can be seen that the same analysis follows through for the real part of the I_{CN}, except that the principle-part integral $-\mathcal{P} \int dE' (E - \varepsilon - E')^{-1}$ appears instead of the factor $i\pi$.

By comparing Eq. (43) to the left-hand side of Eq. (37), we find that the radial equation for the initial wave function is

$$\left(-\frac{\hbar^{2}}{2\mu} \frac{d^{2}}{dR^{2}} + V_{i}(R) + \frac{\hbar^{2}}{2\mu} \frac{J(J+1)}{R^{2}} - E\right) \bar{F}^{J}_{i}(E, R) = i I_{i} - I_{r}, \qquad (44a)$$

where

$$I_{i} = \pi \sum_{J'l} (2J'+1) \begin{pmatrix} J & J' & l \\ 0 & 0 & 0 \end{pmatrix}^{2} \times \int d\varepsilon\, dR' \langle \varepsilon^{+} l | R\rangle^{*} \langle \varepsilon^{+} l | R'\rangle \rho(\varepsilon) \times K_{f}(E'_{0}, J' | R, R') \bar{F}^{J}_{i}(E, R') \qquad (44b)$$

and

$$I_{r} = \sum_{J'l} (2J'+1) \begin{pmatrix} J & J' & l \\ 0 & 0 & 0 \end{pmatrix}^{2} \times \mathcal{P} \int d\varepsilon\, dR'\, dE' \langle \varepsilon^{+} l | R\rangle^{*} \langle \varepsilon^{+} l | R'\rangle \rho(\varepsilon) \times \frac{K_{f}(E', J' | R, R')}{E - \varepsilon - E'} \bar{F}^{J}_{i}(E, R'). \qquad (44c)$$

Although the radial equation has now been determined, it has a nonlocal nature, which considerably complicates a numerical solution. However, it can be converted into a completely local potential by a reasonable approximation which forms the basis the semiclassical analyses. We assume that the major contributions to the integral in Eq. (44) come from regions where the product $F^{J'}_{f}(E', R') \bar{F}^{J}_{i}(E, R')$ is slowly varying. This occurs where the local wave numbers are the same in the initial and final states; i.e., where $k^{J'}_{f}(R') = k^{J}_{i}(R')$ with

$$k^{J}_{s}(R)^{2} = \frac{2\mu}{\hbar^{2}} [E - V_{s}(R)] - \frac{J(J+1)}{R^{2}} .$$

This should be a valid approximation at thermal energies. This condition also implies $\varepsilon + V_{f}(R') = V_{i}(R')$, which is the Franck-Condon principle for the conservation of total electronic energy during a vertical transition. There has even been some experimental evidence that indicate transitions in Penning and associative ionization processes are vertical.[30,31]

If we consider the integral

$$I = \int d\varepsilon \langle \varepsilon^{+} l | R\rangle^{*} \langle \varepsilon^{+} l | R'\rangle \rho(\varepsilon) F^{J'}_{f}(E'_{0}, R) \times F^{J'}_{f}(E'_{0}, R') \bar{F}^{J}_{i}(E, R') \rho(E'_{0}), \qquad (45)$$

which is a factor of I_{i}, and replace $d\varepsilon$ by $-dE'_{0}$, we find that the assumption of vertical transitions implies

$$I \simeq \langle \varepsilon^{+}_{v} l | R\rangle^{*} \langle \varepsilon^{+}_{v} l | R'\rangle \rho(\varepsilon_{v}) \times \int dE'_{0} F^{J'}_{f}(E'_{0}, R) \rho(E'_{0}) F^{J'}_{f}(E'_{0}, R') \bar{F}^{J}_{i}(E, R'), \qquad (46)$$

where $\varepsilon_{v} = \Delta V(R') = V_{i}(R') - V_{f}(R')$. This step does assume that the electron transition amplitude (coupling element) is fairly independent of the energy ε of the ejected electron; i.e.,

$$\langle \varepsilon l | R\rangle \simeq \langle \varepsilon_{v} l | R\rangle . \qquad (47)$$

Computations by Fujii *et al.*, and more-recent ones by Hickman *et al.*, indicate this is reasonably valid.[32,33] Since the final-state nuclear wave functions form a complete set, the previous integral reduces to

$$I = \langle \varepsilon^{+}_{v} l | R\rangle^{*} \langle \varepsilon^{+}_{v} l | R'\rangle \rho(\varepsilon_{v}) \delta(R - R') \bar{F}^{J}_{i}(E, R'). \qquad (48)$$

Using this, the integral I_{i} [Eq. (44b)] becomes

$$I_{i} = \pi \sum_{J'l} (2J'+1) \begin{pmatrix} J & J' & l \\ 0 & 0 & 0 \end{pmatrix}^{2} |\langle \varepsilon^{+}_{v} l | R\rangle|^{2} \times \rho(\varepsilon_{v}) \bar{F}^{J}_{i}(E, R). \qquad (49)$$

With this, we can convert the nonlocal integral into a local form. We can employ the orthogonality relations of the 3*j* symbols and Eq. (B3a) to simplify this

$$I_i=\pi\sum_l |\langle\varepsilon_v^+ l\,|R\rangle|^2\rho(\varepsilon_v)\bar{F}_i^J(E,R)\,. \tag{50}$$

By a similar treatment, we find that term I_r [Eq. (44c)] is

$$I_r=\mathcal{P}\int d\varepsilon\sum_l\frac{|\langle\varepsilon^+ l\,|R\rangle|^2\rho(\varepsilon)}{\varepsilon_v-\varepsilon}\,. \tag{51}$$

Combining these together, we find that the radial equation for the initial channel is approximately

$$\left(-\frac{\hbar^2}{2\mu}\frac{d^2}{dR^2}+V_i(R)+\frac{\hbar^2}{2\mu}\frac{J(J+1)}{R^2}-\frac{i}{2}\Gamma(\varepsilon_v^+|R)\right.$$
$$\left.+\frac{1}{2\pi}\mathcal{P}\int d\varepsilon\frac{\Gamma(\varepsilon^+|R)}{\varepsilon_v-\varepsilon}-E\right)\bar{F}_i^J(E,R)=0\,, \tag{52a}$$

where

$$\Gamma(\varepsilon^\pm|R)=2\pi\sum_l |\langle\varepsilon^\pm l\,|R\rangle|^2\rho(\varepsilon)\,. \tag{52b}$$

This is essentially the same equation obtained by Mori whose analysis was based on Fano's treatment of configuration interactions of discrete states embedded in a continuum of states.[11] The only difference is that the ε in Mori's result is the solution of a transcendental equation that takes level shifts into account. ε_v in Eq. (52a) is the first approximation to this.

To discover the significance of the imaginary part of the potential, we turn to time-dependent quantum theory. The time-dependent wave function of the nuclei in the initial channel is

$$\psi_i(\vec{\mathrm{R}},t)=\exp[-iH_N(\vec{\mathrm{R}})t/\hbar]\chi_d^+(\vec{\mathrm{E}},\vec{\mathrm{R}})\,,$$

where $H_N(\vec{\mathrm{R}})$ is the Hamiltonian for nuclei in Eq. (52). Thus the modulus is

$$|\psi_i(\vec{\mathrm{R}},t)|=\exp\left(-\frac{\Gamma(\varepsilon_v^+|R)t}{2\hbar}\right)|\chi_d^+(\vec{\mathrm{E}},\vec{\mathrm{R}})|. \tag{53}$$

It is apparent that the imaginary part of the potential causes a decay in amplitude as time increases, which means the channel is losing particles. Thus, it is through the complex potential that the inelastic aspect of the collision modifies the initial-channel wave function.

The computation of the level-shift part of the initial-channel potential would necessitate the calculation of a large number of coupling elements at various energies ε for each internuclear separation. However, if we again assume that the coupling elements are fairly independent of the energy of the ejected electron [Eq. (47)] the level shift vanishes,

$$\mathcal{P}\int d\varepsilon\frac{\Gamma(\varepsilon^+|R)}{\varepsilon_v-\varepsilon}\simeq\mathcal{P}\int d\varepsilon\frac{\Gamma(\varepsilon_v^+|R)}{\varepsilon_v-\varepsilon}=0\,. \tag{54}$$

Even when this is not strictly true, the matrix elements between initial and final nuclear wave functions will have dominant contributions at internuclear separations where $\varepsilon=\varepsilon_v=\Delta V(R)$.

In consolidating this discussion of approximations relating to Eq. (44) the radial equation of the initial channel is

$$\left(-\frac{\hbar^2}{2\mu}\frac{d^2}{dR^2}+V_i^T(R)+\frac{\hbar^2}{2\mu}\frac{J(J+1)}{R^2}-E\right)\bar{F}_i^J(E,R)=0\,, \tag{55a}$$

where

$$V_i^T(R)=V_i(R)-\tfrac{1}{2}i\Gamma(R)\,, \tag{55b}$$

$$\Gamma(R)=\Gamma(\varepsilon_v^+|R)=2\pi\sum_l |\langle\varepsilon_v^+ l\,|R\rangle|^2\rho(\varepsilon_v)\,, \tag{55c}$$

and

$$\bar{F}_i^J(E,R)\sim A(E,\mu)\sin(kR-\tfrac{1}{2}J\pi+\bar{\eta}_i^J)\,. \tag{55d}$$

$V_i^T(R)$ is the total approximate complex potential in the initial channel. $\Gamma(R)$ is often called the width of the quasimolecular initial state. It is a measure of the energy spread of the discrete electronic orbitals that must be included in the construction of the metastable state.[34] $\bar{\eta}_i^J$ is the complex phase shift, having both real and imaginary parts. Equation (55) and its solution, $\bar{F}_i^J(E,R)$, will form the standard against which all approximations will be judged. We will refer to its solution as an "exact" solution. [It is exact to the extent that the approximations of Eqs. (46) and (47) are valid.] Now that the radial equations for nuclear motions have been determined [Eqs. (30) and (55)], we can turn to a derivation of differential cross sections in which radial wave functions will be utilized.

IV. DIFFERENTIAL CROSS SECTIONS

The transition rate dw/dq from an initial state i to a final state f per unit interval of the final-state variables $\{q\}$ is[22]

$$\frac{dw}{dq}=\frac{2\pi}{\hbar}|T_{fi}(q)|^2\rho_{\hat{q}}(E_f)\delta_q(E_i-E_f)\,, \tag{56}$$

where $T_{fi}(q)$ is the T matrix defined by Eq. (11). For Penning and associative ionization, the final-state variables $\{q\}$ are $\vec{\varepsilon}$ and $\vec{\mathrm{E}}'$. The coordinate-space representation of the T-matrix elements is

$$T_{fi}(\vec{\mathrm{E}}',\vec{\varepsilon}\,|\vec{\mathrm{E}})=\int d\vec{\mathrm{R}}\,\psi_f^-(\vec{\mathrm{E}}',\vec{\mathrm{R}})^*\langle\vec{\varepsilon}^-|\vec{\mathrm{R}}\rangle\chi_i^+(\vec{\mathrm{E}},\vec{\mathrm{R}})\,. \tag{57}$$

To utilize the results of Sec. III on radial wave functions, we again substitute the partial-wave expansions [Eqs. (26), (27), and (36)] into Eq. (57), note that $Y_{nm}^*(\hat{\Omega})=(-1)^m Y_{n-m}(\hat{\Omega})$ and then use Eqs. (40), (B1b), and (B3c) to obtain

$$T_{fi}=\sum_{J'M'}\sum_{lk}\sum_{JM}(-1)^{J+J'+l}Y_{J'M'}(\hat{\Omega}')Y_{lk}(\hat{\omega})\times Y_{JM}(\hat{\Omega})\langle JJ'l\,|E,E',\varepsilon\rangle\times[(2J+1)(2J'+1)]^{1/2}\times\begin{pmatrix}J & J' & l\\ M & M' & k\end{pmatrix}\begin{pmatrix}J & J' & l\\ 0 & 0 & 0\end{pmatrix},\tag{58a}$$

where

$$\langle JJ'l\,|E,E',\varepsilon\rangle=(i)^{J}(-i)^{J'}\exp(i\bar{\eta}_i^{J})\exp(i\eta_f^{J'})\times\int dR\,F_f^{J'}(E',R)\langle\varepsilon^- l\,|R\rangle\,\bar{F}_i^{J}(E,R).\tag{58b}$$

It is experimentally difficult to measure simultaneously the angular distributions of both the electron and the nuclei in the final state. Thus we will integrate over one of the product angles to determine the total contribution to the remaining angular cross section. We choose to integrate over $\hat{\Omega}'$ (the angle of the product nuclei) to discover the angular differential cross section of the electrons, i.e.,

$$\frac{dw}{d\vec{\varepsilon}}=\int d\vec{E}'\frac{dw}{d\vec{E}'d\vec{\varepsilon}}=\frac{2\pi}{\hbar}\int d\hat{\Omega}'\,|T_{fi}(\vec{E}_0',\vec{\varepsilon}\,|\vec{E})\,|^2\rho(\vec{E}_0')\rho(\vec{\varepsilon}),\tag{59a}$$

where

$$E_0'=E-\varepsilon,\tag{59b}$$

which is the result of the integration $\int dE'$ over the energy-conserving δ function of Eq. (56). Using the orthonormality properties of the spherical harmonics [Eq. (B5a)] the integral over $\hat{\Omega}'$ yields

$$\frac{dw}{d\vec{\varepsilon}}=\frac{2\pi}{\hbar}\sum_{J'M'}(2J'+1)\left|\sum_{JM}\sum_{lk}(2J+1)^{1/2}Y_{JM}(\hat{\Omega})Y_{lk}(\hat{\omega})\langle JJ'l\,|E,E_0',\varepsilon\rangle\begin{pmatrix}J & J' & l\\ 0 & 0 & 0\end{pmatrix}\begin{pmatrix}J & J' & l\\ M & M' & k\end{pmatrix}\right|^2\rho(E_0')\rho(\vec{\varepsilon}).\tag{60}$$

If we choose the incident direction of the nuclei in the initial channel as the z axis of the c.m. coordinate system then $\hat{\Omega}=(\theta_i,\phi_i)=(0,0)$ and

$$\frac{dw}{d\vec{\varepsilon}}=(2\hbar)^{-1}\sum_{J'M'}(2J'+1)\left|\sum_{Jl}(2J+1)\begin{pmatrix}J & J' & l\\ 0 & 0 & 0\end{pmatrix}\begin{pmatrix}J & J' & l\\ 0 & M' & -M'\end{pmatrix}Y_{l-m'}(\hat{\omega})_{\hat{\Omega}}\langle JJ'l\,|E,E_0',\varepsilon\rangle\right|^2\rho(E_0')\rho(\vec{\varepsilon}).\tag{61}$$

The subscript $\hat{\Omega}$ on the spherical harmonic is used to remind us that the angular measurement of $\hat{\omega}$ is made from the incident direction of nuclear motion, $\hat{\Omega}$. This is the formula one would normally use to calculate the angular-energy spectrum of the ejected electron. From Eq. (61), it is apparent that the angular momentum of the ejected electron, l, satisfies two conservation relationships with regard to its projection. Firstly, its projection along the internuclear axis is zero ($m=0$) to conserve the projection of the total electronic angular momentum. Secondly, it acts in concert with the other free particles to conserve their projection of the total orbital angular momentum in the c.m. system.

To obtain the transition rate as a function of electron energy only, we can return to Eq. (60). If we integrate over $\hat{\omega}$, use an orthogonality relation of 3j symbols [Eq. (B3b)] to sum over M' and k, and then employ an orthogonality relationship of spherical harmonics [Eq. (B5b)] to sum over M, we obtain

$$\frac{dw}{d\varepsilon}=(2\hbar)^{-1}\sum_{JJ'l}\left|[(2J'+1)(2J+1)]^{1/2}\begin{pmatrix}J & J' & l\\ 0 & 0 & 0\end{pmatrix}\times\langle JJ'l\,|E,E_0',\varepsilon\rangle\right|^2\rho(E_0')\rho(\varepsilon).\tag{62}$$

It is common to discuss theoretical and experimental results in terms of differential cross sections $d\sigma/dq$. These are related to transitions rates by[22]

$$\frac{d\sigma}{dq}=s_i(f)^{-1}\frac{dw}{dq},\tag{63a}$$

where the flux (f) is given by

$$(f)=|\chi_i^+(\vec{E},\infty)\,|^2v_i=[k_i^2/(2\pi)^3\hbar]\rho(E)^{-1}.\tag{63b}$$

s_i is the statistical weight of the initial state (the probability that the system will be in state i given the experimental procedure employed). v_i is the incident speed of the particles.

Using Eqs. (61) and (63), the angular-energy double-differential cross section for Penning ionization is

$$\frac{d^2\sigma}{d\varepsilon\,d\hat{w}}(E,E')=s_i\frac{4\pi^3}{k_i^2}\sum_{J'M'}\left|\sum_{Jl}\bar{T}^{J}_{J'M'l}(E,E',\hat{\omega})_P\right|^2\times\rho(E')\rho(\vec{\varepsilon})\rho(E),\tag{64a}$$

where

$$\bar{T}^{J}_{J'M'l}(E,E',\hat{\omega})_P=(2J+1)^{1/2}\begin{pmatrix}J & J' & l\\ 0 & M' & -M'\end{pmatrix}\times Y_{l-M'}(\hat{\omega})_{\hat{\Omega}}\,\bar{T}^{J}_{J'l}(E,E')_P,\tag{64b}$$

$$\overline{T}^{J}_{J'l}(E,E')_P=[(2J'+1)(2J+1)]^{1/2}\begin{pmatrix}J & J' & l\\ 0 & 0 & 0\end{pmatrix}\times(i)^J(-i)^l\exp[i(\overline{\eta}^J_i+\sigma^l)]\times\overline{t}^{J}_{J'l}(E,E')_P\,, \tag{64c}$$

$$\overline{t}^{J}_{J'l}(E,E')_P=(-i)^{J'}\exp(i\eta^{J'}_f)\langle F^{J'}_f\langle\varepsilon l\,|R\rangle\overline{F}^{J}_i\rangle\,, \tag{64d}$$

$$\langle F^{J'}_f\langle\varepsilon l\,|R\rangle\overline{F}^{J}_i\rangle=\int dR\,F^{J'}_f(E',R)\times\langle\phi_{\varepsilon l0}|H-E\,|\,\phi_d\rangle\overline{F}^{J}_i(E,R)\,. \tag{64e}$$

The bars over the matrix elements are used to remind us the exact, complex radial wave functions and phase shifts of the entrance channel are employed. We have also dropped the subscript on E'_0 (i.e., $E'\equiv E'_0$), but it is to be understood that these transitions must still be energy conserving ($E=E'+\varepsilon$).

For associative ionization, only discrete values of ε are allowed, since the final nuclear state is discrete. Thus, there is really no differential-energy cross section in this case. However, in any experiment, the measurement of the electron energy has some width $\delta\varepsilon$. By formally integrating the differential cross section represented by Eq. (64a) over such a $\delta\varepsilon$ centered on an allowed energy ε, the energy δ function in $\rho(E')$ produces a discrete cross section. Thus, for associative ionization, the angular differential cross section of the electrons ejected in transitions to a particular vibrational-rotational state (v',J',M') of the molecular ion is

$$\frac{d\sigma}{d\hat{\omega}}(E,v',J',M')=s_i\frac{4\pi^3}{k_i^2}\left|\sum_{Jl}\overline{T}^{J}_{J'M'l}(E,E^{J'}_{v'},\hat{\omega})_A\right|^2\times\rho(\varepsilon)\rho(E)\,, \tag{65}$$

where the matrix elements of associative ionization differ from those of Penning ionization only in that they do not contain the factor $(-i)^{J'}\exp(i\eta^{J'}_f)$ in $\overline{t}^{J}_{J'l}$ [Eq. (64d)]. Equation (64) differs from that given by Koike and Nakamura mainly in the relationship of the phase shifts of the exponential (Eq. (64c)].[6] Apparently, they used a boundary condition of outgoing waves for the final state instead of the appropriate incoming condition [see Eq. (11)]. Note that for the complex potential, the outgoing-wave boundary condition is appropriate [Eq. (25)].

To determine the energy differential cross section for Penning ionization, we use Eqs. (62) and (63) to obtain

$$\frac{d\sigma}{d\varepsilon}(E,E')=s_i\frac{4\pi^3}{k_i^2}\sum_{J'}\sum_{Jl}\left|\overline{T}^{J}_{J'l}(E,E')_P\right|^2\times\rho(E')\rho(\varepsilon)\rho(E)\,. \tag{66}$$

To obtain the formulas appropriate for the cross sections of associative ionizations, we again can formally do an integral over a $\delta\varepsilon$ about an allowed ε. This gives

$$\sigma(E,E^{J'}_{v'})=s_i\frac{4\pi^3}{k_i^2}\sum_{Jl}|\overline{T}^{J}_{J'l}(E,E^{J'}_{v'})_A|^2\rho(\varepsilon)\rho(E)\,. \tag{67}$$

The cross-section formulas given by Eqs. (66) and (67) will be the most accurate discussed in the remainder of this paper. They are exact to the extent that Eq. (55) is exact for the complex potential. Most of the remainder of this paper will concentrate on Penning ionization. Numerical results obtained from approximate formulas, developed below, will be judged in comparison to the exact results obtained from Eq. (66).

Two approximate formulas for the electron energy spectrum will now develop. These will be numerically tested in Sec. V to ascertain their validity. The first approximation will be to replace the complex, entrance-channel wave function, $\overline{F}^J_i(E,R)$, by an approximate form, $F^J_i(E,R)$, that is totally real. $F^J_i(E,R)$ is the solution of the radial equation using only the real part of the potential:

$$\left(-\frac{\hbar^2}{2\mu}\frac{d^2}{dR^2}+V_i(R)+\frac{\hbar^2}{2\mu}\frac{J(J+1)}{R^2}-E\right)F^J_i(E,R)=0\,. \tag{68}$$

One would expect this to be reasonably accurate if the imaginary part of the complex potential, $-\frac{1}{2}\Gamma(R)$, is small compared to the real part, $V_i(R)$. The differential cross section using this approximation is

$$\frac{d\sigma}{d\varepsilon}(E,E')\simeq s_i\frac{4\pi^3}{k_i^2}\sum_{J'}\sum_{Jl}|T^{J}_{J'l}(E,E')_P|^2\times\rho(E')\rho(\varepsilon)\rho(E)\,. \tag{69}$$

The lack of the bar over the T-matrix element indicates that barred quantities in Eqs. (64c)–(64e) are to be replaced by their approximations. F^J_i replaces $\overline{F}^J_i$ in Eqs. (64d) and (64e). The approximate initial-channel phase shift, $\eta^J_i=\lambda^J_i+i\mu^J_i$, replaces $\overline{\eta}^J_i$ in Eq. (64c). (Actually, only μ^J_i is specifically needed, since only the squared modulus of the matrix elements are used.) λ^J_i is readily obtained when $F^J_i(E,R)$ is computed [Eq. (68)].

μ_i^J is an approximate value of $\bar{\mu}_i^J = \mathrm{Im}(\bar{\eta}_i^J)$. To calculate μ_i^J, we employ a perturbation method identical to one used to calculate Born-approximation phase shifts.[35] By multiplying Eq. (55) by F_i^J and Eq. (68) by $\bar{F}_i^J$, subtracting, and then integrating to R', we have

$$\left(F_i^J \frac{d\bar{F}_i^J}{dR} - \bar{F}_i^J \frac{dF_i^J}{dR}\right)_{R=R'} = i\frac{2\mu}{\hbar^2}\int_0^{R'} F_i^J(E,R)\frac{\Gamma(R)}{2}\bar{F}_i^J(E,R)\,. \qquad (70)$$

By extending R' to ∞ and taking the derivatives of the asymptotic forms of the radial wave functions, we have

$$\sinh(\mu_i^J) = \tfrac{1}{2}\pi \int_0^\infty dR\, F_i^J(E,R)\Gamma(R)\bar{F}_i^J(E,R)\rho(E)\,.$$

If we replace F_i^J by its approximate, totally real form, we obtain

$$\sinh(\mu_i^J) \simeq \frac{\pi}{2}\int_0^\infty dR\,[F_i^J(E,R)]^2\Gamma(R)\rho(E) \qquad (71a)$$

or

$$\mu_i^J \simeq \frac{\pi}{2}\int_0^\infty dR\,[F_i^J(E,R)]^2\Gamma(R)\rho(E)\,, \qquad (71b)$$

since we are assuming $\Gamma(R)$ is small in this approximation. This now offers a means of calculating the imaginary part of the complex phase shift without solving the complex-potential radial equation [Eq. (55)]. Simpler classical and semiclassical formulas are also available for the imaginary component of the phase shift.[4,36]

One final approximation will now be made with respect to the energy differential cross section. This will be to average over the effects on the T matrix of the angular momentum of the initial state. This approximation is required for the semiclassical analyses of this and analogous processes.[37,38] This is done by replacing J by its average value. This is just J' since $|J'-l| \leqslant J \leqslant J'+l$. By doing this, we can employ the same technique used to produce Eq. (50), and thereby sum over J in Eq. (69) to obtain

$$\frac{d\sigma}{d\varepsilon}(E,E') \simeq s_i\frac{4\pi^3}{k_i^2}\sum_{J'}(2J'+1)\sum_l |\exp(-\mu_i^J)\langle F_f^J\langle \varepsilon l\,|R\rangle F_i^J\rangle|^2 \times \rho(E')\rho(\varepsilon)\rho(E)\,. \qquad (72)$$

Note that in this approximation, it is assumed that the angular momentum of the nuclei does not change during the transition.

V. NUMERICAL RESULTS FOR He* + H

In this section, we will numerically examine the Penning and associative ionization processes specified by Eqs. (3) and (4). We will consider both the total and differential cross sections associated with a particular thermal kinetic energy in the initial state. In computing cross sections the main problem is to produce the numerical quantum-mechanical wave functions [Eqs. (30) and (55)]. Fortunately, the author had access to computer codes written by Allison that could be modified to construct the required wave functions over the entire region of interest.[39-41] The asymptotic condition for free states is given by Eq. (30b).

The Numerov method was the numerical technique used to integrate the radial equations for the initial- and final-channel wave functions.[42,43] The radial internuclear distance is divided into grid composed of short steps. Starting at some very small internuclear separation, the wave function is integrated outward by taking successive steps along the grid.

We will first consider the computation of a wave function for a channel containing a purely real potential. It is not efficient to use Eq. (30b) to determine the phase shift in the asymptotic region. It is better to write the asymptotic condition as

$$F_s^J(E,R) \sim A(E,\mu)\cos(\eta_s^J)kR \times [j_J(kR) - \tan(\eta_s^J)n_J(kR)]\,, \qquad (73)$$

where $j_J(kR)$ and $n_J(kR)$, being the spherical Bessel and Neumann functions, are exact solutions of the radial equation [Eq. (30a)] for $V_s(R)=0$ at all R. The computed values of $F_s^J(E,R)$ will become proportional to this form when

$$|V_s(R)| \ll \left|E_s - \frac{\hbar^2}{2\mu}\frac{J(J+1)}{R^2}\right|\,. \qquad (74)$$

To determine the phase shift, we have the computer check if the wave function has just gone through zero at each of the grid-point distances (R_n) in the asymptotic region in which we expect the condition above is satisfied. If it has done this at the grid point R_n, we compute the phase shift by

$$\tan(\eta_s^J) = \frac{R_{n-1}W_n j_J(kR_n) - R_n W_{n-1} j_J(kR_{n-1})}{R_n W_{n-1} n_J(kR_{n-1}) - R_{n-1}W_n n_J(kR_n)}\,, \qquad (75)$$

where the W_n are the un-normalized computed values of the wave function. We continue this search until the phase shift has finally converged to within some specified tolerance; in the computations reported here, the tolerance was chosen to be 0.001 rad. The phase shift is then used to normalize properly the computed values of the wave function.

Unlike the problem considered so far, the exact initial-channel radial equation [Eq. (55)] contains a potential that is partly imaginary. If we divide the wave function into real and imaginary parts,

$$\overline{F}_i^J(E,R)=\overline{F}_R^J(E,R)+i\overline{F}_I^J(E,R) \tag{76}$$

and substitute these into Eq. (55), we produce two coupled second-order equations[21]

$$[H(R)-E]\overline{F}_R^J(E,R)=-\tfrac{1}{2}\Gamma(R)\overline{F}_I^J(E,R)\,, \tag{77a}$$

$$[H(R)-E]\overline{F}_I^J(E,R)=\tfrac{1}{2}\Gamma(R)\overline{F}_R^J(E,R)\,, \tag{77b}$$

where

$$H(R)=\left(-\frac{\hbar^2}{2\mu}\frac{d^2}{dR^2}+V_i(R)+\frac{\hbar^2}{2\mu}\frac{J(J+1)}{R^2}\right). \tag{77c}$$

The boundary conditions are

$$\overline{F}_R^J(E,0)=\overline{F}_I^J(E,0)=0 \tag{78a}$$

and

$$\overline{F}_R^J(E,R)\sim A(E,\mu)\cosh(\overline{\mu}_i^J)\sin(kR-\tfrac{1}{2}J\pi+\overline{\lambda}_i^J)\,, \tag{78b}$$

$$\overline{F}_I^J(E,R)\sim A(E,\mu)\sinh(\overline{\mu}_i^J)\cos(kR-\tfrac{1}{2}J\pi+\overline{\lambda}_i^J)\,, \tag{78c}$$

where

$$\overline{\lambda}_i^J=\mathrm{Re}(\overline{\eta}_i^J)\,, \tag{78d}$$

$$\overline{\mu}_i^J=\mathrm{Im}(\overline{\eta}_i^J)\,. \tag{78e}$$

Although more complicated than the real-potential problem owing to the coupling, Allison's computer code utilized a Numerov technique to calculate the phase shifts. In the process, all information needed to construct the complex wave function is computed. Using this information and appropriate formulas,[41] the author modified the code to produce the wave function at each of the grid points R_n. Hickman and Morgner apparently have used a similar method in their computations on the Penning process involving Ar and He*.[44]

Numerical quantum-mechanical computations were conducted for the Penning and associative ionization processes involving metastable helium and atomic hydrogen [Eqs. (3) and (4)]. For this particular process, only the doublet $^2\Sigma$ molecular state produces the ionization. Since a quartet $^4\Sigma$ electronic configuration can also form from the initial atomic species, the appropriate statistical factor is $s_i=2/(2+4)=\frac{1}{3}$. The entrance-channel potential for the HeH*($^2\Sigma^+$) state was determined from a numerical fitting of the values computed by Miller and Schaefer.[45] Although they also computed the HeH$^+$($^1\Sigma$) potential, data calculated by other investigators were used to fit this potential.[46-48] This was done because the asymptotic values obtained by Miller and Schaefer appear to be too small by a factor of approximately 2 compared to the expected behavior.[49] The two potentials used are shown in Fig. 2.

We also need to determine numerical values of the electronic coupling elements, $\langle\varepsilon l\,|R\rangle$, which are transition amplitudes between initial and final states of nuclear motion. The coupling element $\langle\varepsilon_v l\,|R\rangle$ that exists for vertical transitions $[\varepsilon=\varepsilon_v=\Delta V(R)]$ produces essentially the same numerical effect as the more general $\langle\varepsilon l\,|R\rangle$ for two main reasons. One is that coupling element depends only weakly on ε.[32,33] Secondly, the major contribution to the nuclear integrals in the T-matrix elements occur around semiclassical stationary-phase points, R_S, defined by $\varepsilon=\Delta V(R_S)$, the vertical-transition condition.[37,50] It is especially convenient to set $\langle\varepsilon l\,|R\rangle$ equal to $\langle\varepsilon_v l\,|R\rangle$ for the processes considered here [Eqs. (3) and (4)] because Miller, Schaefer, and Slocomb (MSS) computed the values of $\langle\varepsilon_v l\,|R\rangle$ at $R=$2.0, 4.0, 6.0, and 8.0 bohrs for l from zero to nine.[23] The tabulated results of MSS indicate that the $\langle\varepsilon l\,|R\rangle$ are oscillatory functions of both R and l since sign changes occur (Table I of MSS). Such sign changes also appear in the listed results of more-recent calcula-

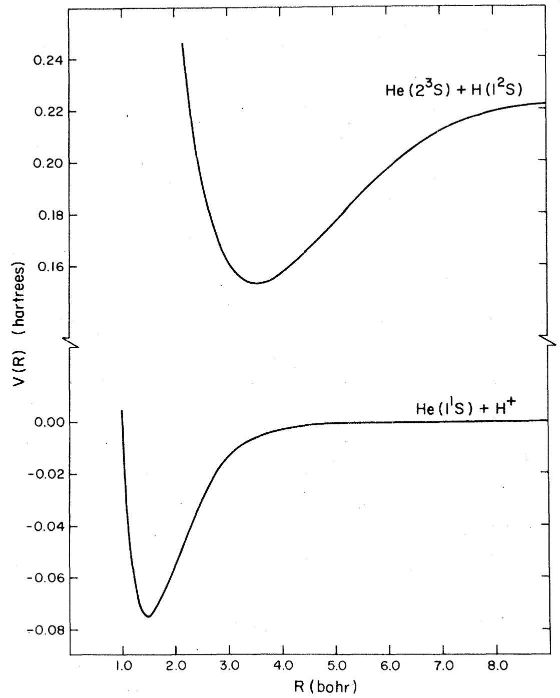

FIG. 2. Intermolecular potentials for Penning and associative ionization involving He(1s2s, 2 ^{3}S) + H(1s, 1 ^{2}S). The upper curve is the potential for the HeH*($^2\Sigma^+$) molecular state, while the lower curve is the potential for the HeH$^+$($^1\Sigma^+$) molecular-ion state. [Atomic units are displayed (Ref. 25): 1 bohr = 0.52917 $\times10^{-8}$ cm; 1 hartree = 4.3595 $\times10^{-11}$ ergs = 27.211 eV.]

tions by Hickman, Isaacson, and Miller (HIM).[33] However, it is obvious that some of the sign changes that appear in these works do not actually occur. For instance, the results of MSS and HIM agree fairly well as to the magnitudes of the coupling elements, but sometimes disagree on the sign. Unfortunately, there appears to be neither uniform agreement nor disagreement in these signs for either constant R or constant l. This problem with signs is even more apparent in the values of the coupling elements given in Tables III and IV of HIM. These represent results of different computational methods of determining the coupling elements. They agree quite well as to magnitudes, but quite often disagree as to sign. The problems may be due to the manner in which the coefficients of the electronic basis sets are numerically calculated. Even for constant R, they may have switched signs (for reasons known only to the computer) as l is varied even though an oscillation is not warranted theoretically.[51] Thus it is not apparent which of the signs changes are spurious, although we expect some oscillations should occur owing to the oscillatory nature of the continuum electronic orbital used in the computations [Eq. (31)]. [In their numerical computations of the imaginary width, both MSS and HIM used Coulomb wave functions to approximate the electronic continuum orbital at all r in Eq. (31); i.e., they set $f^l(\varepsilon,r)=F^l(-k^{-1},kr)$. This and the other numerical approximations just discussed introduce some computational inexactness even in cross sections based on exact formulas.]

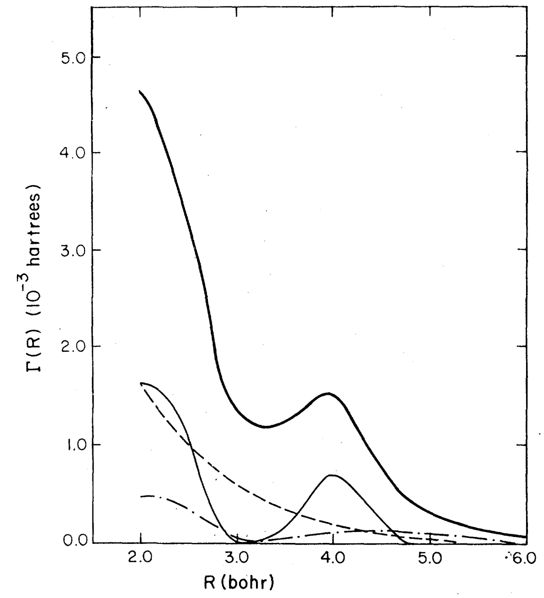

FIG. 3. Magnitude of the imaginary width of the HeH* ($^2\Sigma^+$) molecular state. The contribution from the first three partial waves of the ejected electron are indicated by a dashed line for $l=0$, a light solid line for $l=1$, and a dash-dot line for $l=2$. The heavy solid line is the total width, obtained from the sum of the contributions of $l=0$ to 9. [Atomic units are displayed (Ref. 25): 1 bohr $=0.52917\times10^{-8}$ cm; 1 hartree $=4.3595\times10^{-11}$ ergs $=27.211$ eV.] For $R>6.0$ bohrs, the width is adequately given by $\Gamma(R)=0.09\exp(-1.13R)$ in hartrees.

In the calculations presented here, we will employ the values of the coupling elements given by MSS. At least for $\langle\varepsilon 0|R\rangle$, the oscillation in R given in MSS is more consistent with the wavelength of the ejected electron than is that given in HIM. A separate numerical fit of $\langle\varepsilon l|R\rangle$ as a function of R was made for points between 2.0, 4.0, 6.0, and 8.0 bohrs. Since these functions oscillate as a function of R, they can produce an undulatory pattern in the total width of the channel [Eq. (73c)]. This is seen in Fig. 3, which displays the total width and the contributions from the three partial waves of the ejected electron. Previous investigators have only used a width that is a smooth fit of the computed values for the total width at $R=2.0$, 4.0, 6.0, and 8.0 bohrs.[23,52] If the dips were there, they would be missed by this method. Such dips will have their most-pronounced effect in the energy differential cross section. As has been discussed elsewhere, the magnitude of the differential cross section is mainly determined by the values of the coupling elements at two points of stationary phase that depend on electron energy.[37] For stationary points in the undulatory regions of the width, the absolute magnitude of the energy differential cross section may be affected significantly if such undulations do occur.

However, it should not be inferred from Fig. 3 that the undulation appearing around $R=3.5$ bohrs must be there in physical reality; the oscillatory structure of $\langle\varepsilon l|R\rangle$ cannot be unambiguously determined from published values. [The more accurate values of $\Gamma(R)$ reported in HIM at $R=2.0$, 2.5, 3.0, 3.5, and 4.0 bohrs indicate that it does not really exist.] However, the issue of whether or not such undulations exist for the particular Penning and associative ionization processes examined here will not affect the intent or conclusions of this paper. Yet these considerations should indicate that undulations may exist in the imaginary widths of other systems and processes.

The actual numerical computations using the complex potential were done for an incident nuclear kinetic energy of 0.00184 hartrees (0.050 eV). This energy was chosen because it was the typical incident energy involved in the experimental measurements of the electron energy distribution.[53,54] Although the main thrust of this paper is the calculation and interpretation of ejected-particle energy distributions, we begin our investigation with an examination of total elastic and inelastic cross sections. To compute these, we only need the complex phase shifts of the entrance channel. The total elastic and inelastic cross sections are[21, 55]

$$\sigma_{\mathrm{el}}=\frac{\pi}{k_i^2}\sum_J (2J+1)\,|1-S_e^J|^2\,, \tag{79a}$$

$$\sigma_{\mathrm{in}}=\frac{\pi}{k_i^2}\sum_J (2J+1)(1-|S_e^J|^2)\,, \tag{79b}$$

where S_e^J is the S matrix associated with elastic scattering. This is related to the initial-channel phase shifts by $S_e^J=\exp(2i\bar{\eta}_i^J)=\exp(2i\bar{\lambda}_i^J)\exp(-2\bar{\mu}_i^J)$.

Wave functions and corresponding complex phase shifts were computed for values of J up to 60, where the real and imaginary parts of the initial-channel phase shift become effectively zero. This diminishment of the phase shift is owing to the fact that the penetration of the centrifugal barrier begins at $J=26$ for the incident energy we are using. As the angular momentum increases, the wave function penetrates the barrier less and less. Since the wave function correspondingly feels less and less of the effects of the interior potential (where the real and imaginary parts are large), the real and imaginary parts of the complex phase shifts go to zero. The computed total elastic cross section is $\sigma_{\mathrm{el}}=255.67$ bohr^2 (7.1601×10^{-15} cm^2) and the total inelastic is $\sigma_{\mathrm{in}}=105.27$ bohr^2 (2.9481×10^{-15} cm^2). This is in agreement with the inelastic cross section obtained by Cohen and Lane (3.0×10^{-15} cm^2) in their complex-potential computation.[52] Although inadequate to compute the electron energy spectrum, even simple classical dynamical models can produce nearly the same result for the total cross section.[23] The computational result is consistent with the experimental cross section obtained by Morgner (120 ± 20 bohr^2) at the same average kinetic energy of 0.05 eV.[56] (For a review of experimental measurements on Penning ionization, see Ref. 57.)

We can now begin to compare the exact calculation with the approximate results achieved by employing the wave function $F_i^J(E,R)$, which is computed using only the real part of the potential [Eq. (68)]. Since the imaginary part of the complex potential is much smaller than the real part (compare Figs. 2 and 3), we expect that the initial-channel wave functions will not be greatly perturbed by the presence of the imaginary width. To verify this, we first examine the phase shifts in detail. For nearly all values of the angular momentum, the totally real phase shift of $F_i^J(E,R)$ equals the real part of the complex phase shift, to within the convergence tolerance of 0.001 rad. The only significant deviation occurred for J values just prior to barrier penetration. At $J=21$, the difference in these phase shifts was 0.006, and at $J=26$ it was at its maximum of 0.059. For $J=27$ and greater, there was again no difference within the tolerance. This is consistent with the effects one might expect by considering the relative magnitude of the width in comparison to the other terms in the radial equation. When the imaginary part of the entrance-channel potential is much smaller than the other terms in the radial wave equation

$$\left|\frac{\Gamma}{2}(R)\right| \ll \left|E-V_i(R)-\frac{\hbar^2}{2\mu}\frac{J(J+1)}{R^2}\right|\,, \tag{80}$$

we expect that the imaginary part of the potential will have only a relatively small effect on the wave function. In the process we are considering here, $|\frac{1}{2}\Gamma(R)|\ll V_i(R)$ everywhere.

Thus, the condition above is usually not met only around classical turning points where the term on the right-hand side is zero. Near the interior turning point of the entrance channel, the potential is rapidly changing. Consequently, the condition expressed by Eq. (80) is not satisfied only within a small region about the turning point. In this case then, the imaginary width of the potential $[\frac{1}{2}\Gamma(R)]$ will only have a small overall effect. The effects of the turning points of the centrifugal barrier should be larger since the barrier spans a greater distance. The condition of Eq. (80) may then not be met over a significant range of internuclear separation about the peak of the barrier for values of J near the onset of barrier penetration. This is precisely what occurs in the approximate, real phase shifts between $J=21$ and $J=26$ (which is when barrier penetration occurs). A similar deviation in the approximate, imaginary phase shift [Eq. (71)] occurs in comparison to the imaginary part of the complex phase shift of $\bar{F}_i^J(E,R)$. Only in this case though, the error begins at $J=24$ with a difference of 0.004 rad and increases to a maximum of 0.032 at $J=26$. (The imaginary part of the complex phase shift, $\bar{\lambda}_i^J$, is fairly constant until penetration begins, having a typical value of 0.337.) Again, there is no deviation for larger angular momentum.

Even though these deviations exist, they are not particularly large. This implies that the entrance-channel wave function may not be greatly affected by the presence of the small imaginary width. We should then be able to estimate the effect of this width on cross sections by only considering the totally real, approximate wave function [Eq. (68)]. To probe this possibility, we return to Eq. (77). If the condition of Eq. (80) is satisfied nearly everywhere, the equations for the real part [Eq. (77a)] and the imaginary part [Eq. (77b)] of $\bar{F}_i^J(E,R)$ are essentially decoupled. Since both

$\bar{F}_R^J(E,R)$ and $\bar{F}_I^J(E,R)$ then satisfy nearly the same equation, their ratio over almost the entire range of R should be largely determined by their asymptotic conditions [Eqs. (78b) and (78c)]. (We expect this should breakdown near classical turning points.)

Consequently, we expect $\bar{F}_R^J(E,R)$ and $\bar{F}_I^J(E,R)$ to be out of phase with respect to one another by $\frac{1}{2}\pi$ rad, even in the nonasymptotic interior region of the potential. This was verified for typical angular momenta by a direct examination of the computed real and imaginary parts of the wave function. This also shows up in the contribution to the T-matrix elements from $\bar{F}_R^J(E,R)$ and $\bar{F}_I^J(E,R)$. For fixed l, J', and E', the real and imaginary contributions to $T_{J',l}^J(E,E')$ oscillate between positive and negative for increasing J. This happens because the main contribution to the elements of fixed E and E' occurs around a stationary-phase point that is largely independent of J.[37] As J changes, the local phases of $\bar{F}_R^J$ and $\bar{F}_I^J$ also change owing to the centrifugal term in the effective potential. Thus the values of these component wave functions around the stationary-phase point oscillate as a function of J. These oscillations are reflected in the matrix elements. The contribution from $\bar{F}_R^J(E,R)$ is large when that from $\bar{F}_I^J(E,R)$ is small, and vice versa. This means that the contributions are out of phase by about $\frac{1}{2}\pi$, since the final-state wave function is the same for both contributions. This is precisely what one would expect if the wave functions are also out of phase by this amount.

A second hypothesis that we can suggest from the asymptotic condition concerns the relative size of the contributions from the real and imaginary parts of $\bar{F}_i^J(E,R)$. By noting that

$$|\langle \bar{F}_i^J\langle \epsilon l|R\rangle F_f^{J'}\rangle|^2 = |\langle \bar{F}_R^J\langle \epsilon l|R\rangle F_f^{J'}\rangle|^2 + |\langle \bar{F}_I^J\langle \epsilon l|R\rangle F_f^{J'}\rangle|^2 \qquad (81)$$

we see that the imaginary part will increase the magnitude of the T-matrix elements as long as the contribution from the real part is not significantly decreased. Again, by direct examination of the T-matrix elements, the contribution from the real part of the wave function is within a few percent of the value obtained using the approximate wave function produced by only the real potential. [This was also indicated by how well the totally real, approximate wave function, $F_i^J(E,R)$, worked in phase shift calculations.] This part of the T matrix is, therefore, not significantly affected by changes in the real part of the radial wave function even in the presence of the imaginary potential. From these considerations, the average fractional contribution of the imaginary component to the T-matrix elements should be given by

$$\frac{|\langle \bar{F}_I^J\langle \epsilon l|R\rangle F_f^{J'}\rangle|^2_{\text{av}}}{|\langle \bar{F}_i^J\langle \epsilon l|R\rangle F_f^{J'}\rangle|^2_{\text{av}}} \simeq \frac{\sinh^2(\bar{\mu}_i^J)}{\cosh^2(\bar{\mu}_i^J)+\sinh^2(\bar{\mu}_i^J)}. \qquad (82)$$

Using a typical value of the imaginary phase shift (0.337) prior to barrier penetration, this ratio is about 0.1. By neglecting the contribution from $\bar{F}_I^J(E,R)$, which we do in the approximate energy differential cross section of Eq. (69), we expect to introduce an error of about 10%.

In Fig. 4, we compare the energy differential cross section obtained using the complex radial wave function [Eq. (66)] and the approximate real wave function [Eq. (69)]. As expected the exact results are generally larger than the approximate. The maximum error in the approximate result is 8%, with a typical error being 5%. This is quite consistent with the 10% deviation predicted from Eq. (82). We thus conclude that relative contributions of the real and imaginary parts of the initial-channel wave function are indeed determined mainly by their asymptotic conditions when the imagi-

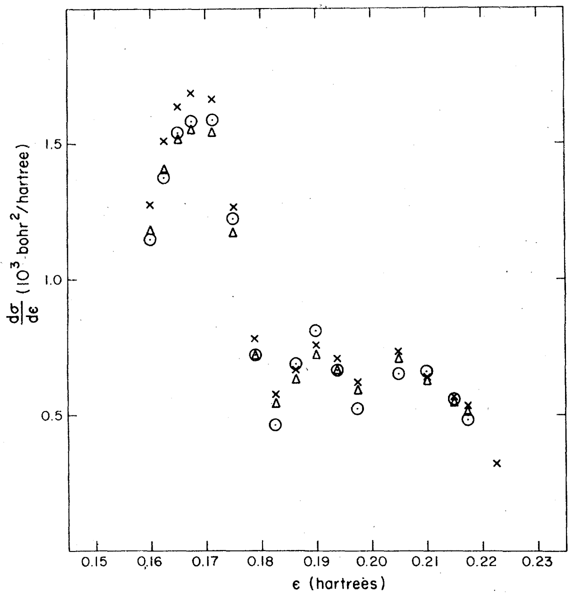

FIG. 4. Comparison of the energy differential cross sections of ejected electrons from Penning ionization [Eq.(3)], computed using three levels of approximation. Crosses indicate results obtained by using exact, complex radial wave functions in T-matrix elements [Eq. (66)]; triangles are results using totally real, radial wave functions [Eq.(69)]; circled dots are results using totally real, radial wave functions with average angular momenta ($J=J'$) [Eq.(72)]. [Atomic units are displayed (Ref. 25): 1 hartree$=4.3595\times10^{-11}$ ergs; 1 bohr^2/hartree $=6.4232\times10^{-7}$ cm^2/erg$=1.029\times10^{-18}$ cm^2/eV.] The initial kinetic energy of the colliding nuclei is $E=0.001\,84$ hartree$=0.050$ eV.

nary width of the potential is small [Eq. (80)] nearly everywhere.

This approach can be used to estimate the matrix elements involving $\bar{F}_I^J$ even if only the approximate, real wave function F_i^J is computed [Eq. (68)]. We know F_i^J nearly equals $\bar{F}_R^J$. Consequently, the relative sizes of the average values of the matrix elements are given by

$$\frac{|\langle \bar{F}_I^J \langle \varepsilon l \,|R\rangle F_f^{J'} \rangle|_{\mathrm{av}}^2}{|\langle F_i^J \langle \varepsilon l \,|R\rangle F_f^{J'} \rangle|_{\mathrm{av}}^2} \simeq \frac{\sinh^2(\mu_i^J)}{\cosh^2(\mu_i^J)} . \tag{83}$$

We can push this even further by employing the knowledge that the imaginary and real contributions are $\frac{1}{2}\pi$ out of phase with respect to one another. Suppose that $|\langle F_i^J \langle \varepsilon l \,|R\rangle F_f^{J'} \rangle|^2$ has two consecutive maxima at $J=J_1$ and $J=J_2$, with an intervening minima at $J=j$. Since the matrix elements of $\bar{F}_I^J$ are about $\frac{1}{2}\pi$ out of phase with those of F_i^J, $|\langle \bar{F}_I^J \langle \varepsilon l \,|R\rangle F_f^{J'} \rangle|^2$ should be near a maximum at $J=j$. We can estimate its magnitude as

$$\begin{aligned} |\langle \bar{F}_I^j \langle \varepsilon l \,|R\rangle F_f^{J'} \rangle|^2 \simeq & \frac{1}{2} \frac{\sinh^2(\mu_i^j)}{\cosh^2(\mu_i^j)} \\ & \times (|\langle F_i^{J_1} \langle \varepsilon l \,|R\rangle F_f^{J'} \rangle|^2 \\ & + |\langle F_i^{J_2} \langle \varepsilon l \,|R\rangle F_f^{J'} \rangle|^2) . \end{aligned} \tag{84}$$

Consecutive approximate values of these matrix-element maxima can be used to estimate $|\langle \bar{F}_I^J \langle \varepsilon l \,|R\rangle F_f^{J'} \rangle|^2$ for values of J in between the j's.

The final approximation we investigate is that of replacing the angular momentum of the initial state of nuclear motion, J, by its average value, J'. This approximation leads to Eq. (72) as the formula for the differential cross section. As previously mentioned, this step is generally required if one wishes to employ JWKB semiclassical approximations. The cross section that results from Eq. (72) is also displayed in Fig. 4. The maximum deviation from the exact computation is 20%, with a typical value of 10%. Although this error is larger than the previous approximation, it is still quite tolerable for many applications. (This error will of course be smaller for processes in which less l of the electronic transition are significant.) It is particularly interesting and useful that this approximation, like the prior one, correctly reproduces the positions of the extrema of the oscillatory structure. This can lead to a detailed semiclassical analysis of the source of this structure, which is analogous to that employed in elastic angular scattering near a rainbow extremum.[37] The simpler and more-intuitive semiclassical results are in good agreement with the quantum-mechanical results reported here.

As the final computation of this paper, we present the individual cross sections of associative ionization (summed over M') to each of the 149 bound states of $\mathrm{HeH}^+(^1\Sigma^+)$, using exact formulas [Eq. (67), but again employing the numerical approximations discussed after Eq. (78)]. The incident kinetic energy of the colliding nuclei is $E = 0.001\,84$ hartree (0.050 eV). The bound-state eigenenergies and eigenfunctions of HeH^+ were computed using a Numerov technique that matched solutions of outgoing and incoming numerical integrations.[42] The resulting energies and cross sections are given in Table I. At the incident energy considered here, the $v'=2$, 3, and 4 vibrational levels of HeH^+ are preferentially populated as a result of associative ionization.

VI. CONCLUSION

The main conclusion that we can draw from these numerical results is that the effects of the imaginary width of the complex potential can be rather accurately determined from computations dealing with only the real part of the potential—as long as the width is small compared to the other energy terms [Eq. (81)]. The totally real, approximate wave functions [the solutions of Eq. (68)] give quite accurate values for the real part of the complex phase shifts. Using a perturbation technique [Eq. (71)], these approximate wave functions yield accurate values for the imaginary part of the complex phase shifts. These can be used in turn to compute total elastic and inelastic cross sections [Eq. (79)]. We have found that the ratios of the magnitudes of the real and imaginary components of the complex wave functions are largely determined by their asymptotic forms. Both their local values and their overall effects (as revealed by matrix elements) are generally $\frac{1}{2}\pi$ out of phase. This can be used to make a reasonable estimate of the contribution owing to the imaginary part of the complex wave functions to the transition matrix elements [Eqs. (83) and (84)]. However, all these results are dependent upon the imaginary width of the complex potential being much less than the real part. When the imaginary part becomes comparable to the real, such as in the associative detachment process $\mathrm{H} + \mathrm{H}^- \rightarrow \mathrm{H}_2 + e^-$, the approximate formulas for cross sections to individual final states [e.g., Eq. (69)] are many orders of magnitude in error.[58] In such cases, only exact formulas [Eqs. (66) and (67)] will work.

ACKNOWLEDGMENTS

Most of the research of this project was conducted while the author was a NSF Predoctoral Fellow at Harvard University and the Center for Astrophysics, Cambridge, Mass. Additional sup-

TABLE I. Cross sections of associative ionization [Eq. (4)] to individual rotational-vibrational states of the molecular ion HeH$^+$ ($^1\Sigma^+$). J' is the rotational quantum number and v' is the vibrational quantum number. $E_{v'}^{J'}$ is the eigenenergy of the (v', J') state (1 hartree = 4.3595×10^{-11} ergs = 27.211 eV). $\sigma(E, E_{v'}^{J'})$ is the cross section to the (v', J') state, summed over the degenerate magnetic quantum numbers M' [Eq. (67)]. (1 bohr^2 = 2.8002×10^{-17} cm^2.) The initial kinetic energy of the colliding nuclei is E=0.001 84 hartree = 0.050 eV.

J'	v'	$E_{v'}^{J'}$ (hartrees)	$\sigma(E, E_{v'}^{J'})$ (bohr^2)
0	0	-6.7711 (-02)	6.7310 (-06)
	1	-5.3837 (-02)	2.2415 (-04)
	2	-4.0509 (-02)	2.9877 (-03)
	3	-2.8912 (-02)	1.6107 (-02)
	4	-1.9786 (-02)	1.4332 (-02)
	5	-1.2616 (-02)	3.5847 (-03)
	6	-7.3465 (-03)	1.7365 (-03)
	7	-3.8044 (-03)	3.8678 (-03)
	8	-1.6781 (-03)	2.3602 (-03)
	9	-5.5516 (-04)	1.0697 (-03)
	10	-7.3129 (-05)	1.8901 (-04)
1	0	-6.7404 (-02)	2.0590 (-05)
	1	-5.3546 (-02)	6.8362 (-04)
	2	-4.0235 (-02)	9.1027 (-03)
	3	-2.8667 (-02)	4.8773 (-02)
	4	-1.9581 (-02)	4.2229 (-02)
	5	-1.2442 (-02)	1.1354 (-02)
	6	-7.2088 (-03)	4.6790 (-03)
	7	-3.7046 (-03)	1.1161 (-02)
	8	-1.6127 (-03)	6.9711 (-03)
	9	-5.1581 (-04)	3.1897 (-03)
	10	-5.8496 (-05)	5.0146 (-04)
2	0	-6.6792 (-02)	3.5676 (-05)
	1	-5.2966 (-02)	1.1775 (-03)
	2	-3.9689 (-02)	1.5646 (-02)
	3	-2.8180 (-02)	8.2786 (-02)
	4	-1.9172 (-02)	6.7778 (-02)
	5	-1.2095 (-02)	2.0944 (-02)
	6	-6.9361 (-03)	6.1609 (-03)
	7	-3.5075 (-03)	1.7055 (-02)
	8	-1.4843 (-03)	1.1151 (-02)
	9	-4.3932 (-04)	5.1870 (-03)
3	0	-6.5878 (-02)	5.2923 (-05)
	1	-5.2098 (-02)	1.7316 (-03)
	2	-3.8875 (-02)	2.2937 (-02)
	3	-2.7455 (-02)	1.1902 (-01)
	4	-1.8564 (-02)	8.9283 (-02)
	5	-1.1582 (-02)	3.3596 (-02)
	6	-6.5337 (-03)	5.6845 (-03)
	7	-3.2182 (-03)	2.0447 (-02)
	8	-1.2976 (-03)	1.4300 (-02)
	9	-3.3018 (-04)	6.7759 (-03)
4	0	-6.4667 (-02)	7.3461 (-05)
	1	-5.0949 (-02)	2.3767 (-03)
	2	-3.7798 (-02)	3.1349 (-02)
	3	-2.6499 (-02)	1.5830 (-01)
	4	-1.7765 (-02)	1.0493 (-01)
	5	-1.0912 (-02)	5.0443 (-02)
	6	-6.0103 (-03)	3.5746 (-03)
	7	-2.8447 (-03)	2.0258 (-02)
	8	-1.0599 (-03)	1.5504 (-02)
	9	-1.9547 (-04)	7.4084 (-03)
5	0	-6.3166 (-02)	9.8713 (-05)
	1	-4.9524 (-02)	3.1512 (-03)
	2	-3.6466 (-02)	4.1334 (-02)
	3	-2.5323 (-02)	2.0133 (-01)
	4	-1.6781 (-02)	1.1287 (-01)
	5	-1.0095 (-02)	7.2151 (-02)
	6	-5.3776 (-03)	1.3824 (-03)
	7	-2.3986 (-03)	1.6025 (-02)
	8	-7.8151 (-04)	1.3833 (-02)
	9	-4.7672 (-05)	6.1675 (-03)
6	0	-6.1383 (-02)	1.3054 (-04)
	1	-4.7829 (-02)	4.1047 (-03)
	2	-3.4889 (-02)	5.3464 (-02)
	3	-2.3938 (-02)	2.4854 (-01)
	4	-1.5623 (-02)	1.1145 (-01)
	5	-9.1440 (-03)	9.8309 (-02)
	6	-4.6511 (-03)	2.0198 (-03)
	7	-1.8959 (-03)	8.9076 (-03)
	8	-4.7687 (-04)	9.1971 (-03)
7	0	-5.9327 (-02)	1.7141 (-04)
	1	-4.5873 (-02)	5.3040 (-03)
	2	-3.3076 (-02)	6.8474 (-02)
	3	-2.2359 (-02)	2.9988 (-01)
	4	-1.4303 (-02)	9.9767 (-02)
	5	-8.0760 (-03)	1.2663 (-01)
	6	-3.8490 (-03)	9.1062 (-03)
	7	-1.3567 (-03)	2.4158 (-03)
	8	-1.6580 (-04)	3.5278 (-03)
8	0	-5.7008 (-02)	2.2477 (-04)
	1	-4.3666 (-02)	6.8410 (-03)
	2	-3.1041 (-02)	8.7330 (-02)
	3	-2.0602 (-02)	3.5446 (-01)
	4	-1.2833 (-02)	7.8345 (-02)
	5	-6.9075 (-03)	1.5219 (-01)
	6	-2.9923 (-03)	2.5066 (-02)
	7	-8.0542 (-04)	1.3073 (-03)
9	0	-5.4438 (-02)	2.9520 (-04)
	1	-4.1219 (-02)	8.8428 (-03)
	2	-2.8798 (-02)	1.1128 (-01)
	3	-1.8687 (-02)	4.0994 (-01)
	4	-1.1229 (-02)	5.0230 (-02)
	5	-5.6571 (-03)	1.6717 (-01)
	6	-2.1037 (-03)	4.8114 (-02)
	7	-2.6926 (-04)	7.6252 (-03)
10	0	-5.1629 (-02)	3.8907 (-04)
	1	-3.8542 (-02)	1.1489 (-02)
	2	-2.6364 (-02)	1.4191 (-01)
	3	-1.6633 (-02)	4.6187 (-01)
	4	-9.5092 (-03)	2.2155 (-02)
	5	-4.3453 (-03)	1.6212 (-01)
	6	-1.2088 (-03)	6.9376 (-02)

TABLE I. (*Continued*)

J'	v'	$E_{v'}^{J'}$ (hartrees)	$\sigma(E, E_{v'}^{J'})$ (bohr^2)	J'	v'	$E_{v'}^{J'}$ (hartrees)	$\sigma(E,E_{v'}^{J'})$ (bohr^2)
11	0	-4.8595 (-02)	5.1503 (-04)	16	0	-3.0522 (-02)	2.3229 (-03)
	1	-3.5650 (-02)	1.5031 (-02)		1	-1.8523 (-02)	6.9147 (-02)
	2	-2.3755 (-02)	1.8122 (-01)		2	-8.9243 (-03)	5.9156 (-01)
	3	-1.4462 (-02)	5.0309 (-01)		3	-2.5586 (-03)	2.2409 (-01)
	4	-7.6987 (-03)	5.0813 (-03)				
	5	-2.9971 (-03)	1.3006 (-01)	17	0	-2.6427 (-02)	3.2352 (-03)
	6	-3.4157 (-04)	7.3102 (-02)		1	-1.4709 (-02)	9.8541 (-02)
					2	-5.8161 (-03)	7.0619 (-01)
12	0	-4.5348 (-02)	6.8505 (-04)		3	-1.4576 (-04)	8.2398 (-02)
	1	-3.2556 (-02)	1.9838 (-02)				
	2	-2.0993 (-02)	2.3159 (-01)	18	0	-2.2205 (-02)	4.5565 (-03)
	3	-1.2195 (-02)	5.2384 (-01)		1	-1.0827 (-02)	1.4250 (-01)
	4	-5.8281 (-03)	1.2417 (-02)		2	-2.7491 (-03)	7.8837 (-01)
	5	-1.6464 (-03)	7.4974 (-02)				
				19	0	-1.7871 (-02)	6.5606 (-03)
13	0	-4.1904 (-02)	9.1648 (-04)		1	-6.9162 (-03)	2.1037 (-01)
	1	-2.9278 (-02)	2.6469 (-02)				
	2	-1.8100 (-02)	2.9582 (-01)	20	0	-1.3440 (-02)	9.7414 (-03)
	3	-9.8502 (-03)	5.1304 (-01)		1	-3.0228 (-03)	3.1659 (-01)
	4	-3.9355 (-03)	5.3632 (-02)				
	5	-3.4295 (-04)	2.0677 (-02)	21	0	-8.9305 (-03)	1.4665 (-02)
14	0	-3.8275 (-02)	1.2360 (-03)	22	0	-4.3607 (-03)	2.2911 (-02)
	1	-2.5832 (-02)	3.5817 (-02)				
	2	-1.5103 (-02)	3.7690 (-01)				
	3	-7.4481 (-03)	4.6070 (-01)				
	4	-2.0655 (-03)	1.2301 (-01)				
15	0	-3.4476 (-02)	1.6847 (-03)				
	1	-2.2240 (-02)	4.9311 (-02)				
	2	-1.2033 (-02)	4.7662 (-01)				
	3	-5.0083 (-03)	3.6179 (-01)				
	4	-2.6951 (-04)	1.8830 (-01)				

port for this work was received from the Air Force Office of Scientific Research (AFOSR 71-2132) and the National Aeronautics and Space Administration (NASA NGL 22007-136). The author would like to express his indebtedness to A. Dalgarno, Harvard University and Center for Astrophysics, for his many helpful discussions and suggestions concerning the subject of this paper. The author would also like to thank A. Allison, University of Glasgow, who, with patience and understanding, tutored the author through his novice years of writing large-scale computer codes.

APPENDIX A: NORMALIZATION OF A CONTINUUM STATE

If $\{\psi(x,y)\}$ is a complete set of functions with continuous variables x and y, then the proper orthonormality relations are[59]

$$\int \psi^*(x',y)\rho(x,y)\psi(x,y)\,dy=\delta(x-x')\,, \tag{A1a}$$

$$\int \psi^*(x,y')\rho(x,y)\psi(x,y)\,dx=\delta(y-y')\,. \tag{A1b}$$

$\rho(x,y)$ is the density of the functions.

Consider a continuum wave function of the form

$$\psi(\vec{E},\vec{R})=[\mu k/\hbar^2(2\pi)^3]^{1/2}e^{i\vec{k}\cdot\vec{R}}\,, \tag{A2a}$$

where

$$\vec{k}=[(2\mu/\hbar^2)E]^{1/2}\hat{\Omega}\,. \tag{A2b}$$

Letting $x=\vec{E}$ and $y=\vec{R}$, we have

$$\begin{aligned}\int \psi^*(\vec{E}',\vec{R})\psi(\vec{E},\vec{R})\,d\vec{R} &= [\mu k/\hbar^2(2\pi)^3](2\pi)^3\delta(\vec{k}-\vec{k}')\\ &=(\mu k/\hbar^2)[\delta(k-k')/k^2]\delta(\hat{\Omega}-\hat{\Omega}')\\ &=\frac{\mu}{\hbar^2 k}\left(\frac{d(k-k')}{dE}\right)^{-1}\delta(E-E')\delta(\hat{\Omega}-\hat{\Omega}')\\ &=\delta(E-E')\delta(\hat{\Omega}-\hat{\Omega}')=\delta(\vec{E}-\vec{E}')\,.\end{aligned} \tag{A3}$$

Likewise

$$\int \psi^*(\vec{E},\vec{R}')\psi(\vec{E},\vec{R})\,d\vec{E}$$

$$= \int \frac{\mu k}{\hbar^2(2\pi)^3}\exp[i\vec{k}\cdot(\vec{R}-\vec{R}')\,dE\,d\hat{\Omega}$$

$$= \frac{1}{(2\pi)^3}\int \exp[i\vec{k}\cdot(\vec{R}-\vec{R}')]d\vec{k}$$

$$= \delta(\vec{R}-\vec{R}')\,. \qquad \text{(A4)}$$

Thus, $\psi(\vec{E},\vec{R})$, specified by Eq. (A2), is an energy- and space-normalized wave function with $\rho(\vec{E}) = \rho(\vec{R}) = 1$.

We can make a partial-wave expansion of $\exp(i\vec{k}\cdot\vec{R})$ to obtain[55]

$$\psi(\vec{E},\vec{R}) = \left(\frac{\mu k}{\hbar^2(2\pi)^3}\right)^{1/2}(4\pi)\sum_{lm} Y^*_{lm}(\hat{\Omega})Y_{lm}(\hat{R}) \times (i)^l j_l(kR)R^{-1}\,, \qquad \text{(A5)}$$

where $j_l(kR)$, the spherical Bessel function, is related to the ordinary Bessel functions by

$$j_l(kR) = (\pi R/2k)^{1/2}J_{l+1/2}(kR)\,. \qquad \text{(A6)}$$

Thus

$$\psi(\vec{E},\vec{R}) = \sum_{lm} Y^*_{lM}(\hat{\Omega})Y_{lm}(\hat{R})(i)^l F^l(E,R)\,, \qquad \text{(A7a)}$$

where

$$F^l(E,R) = (2\mu/\pi\hbar^2 k)^{1/2}kj_l(kR)\,. \qquad \text{(A7b)}$$

In Eqs. (A7), we have shifted the normalization coefficient into the radial function $F^l(E,R)$.

It can be shown that the same analysis holds true for wave functions produced by the scattering of a plane wave off a central potential.[60] In this case

$$\psi(\vec{E},\vec{R}) = [\mu k/\hbar^2(2\pi)^3]^{1/2} \times [\exp(i\vec{k}\cdot\vec{R}) + f(\theta)\exp(ikR)R^{-1}]$$

$$= \sum_{JM} Y^*_{JM}(\hat{\Omega})Y_{JM}(\hat{R})(i)^J \times \exp(i\eta^J)F^J(E,R)\,, \qquad \text{(A8a)}$$

where asymptotically

$$F^J(E,R) \sim (2\mu/\pi\hbar^2 k)^{1/2}\sin(kR - \tfrac{1}{2}J\pi + \eta^J)\,. \qquad \text{(A8b)}$$

With this normalization, the density of states is still

$$\rho(\vec{R}) = 1 \qquad \text{(A9a)}$$

and

$$\rho(\vec{E}) = 1\,. \qquad \text{(A9b)}$$

For convenience, we can make

$$\rho(E) = \rho(\hat{\Omega}) = \rho(R) = \rho(\hat{R}) = 1\,. \qquad \text{(A10)}$$

APPENDIX B: RELATIONSHIPS INVOLVING *D* MATRICES, 3*j* SYMBOLS, AND SPHERICAL HARMONICS

(i) *D*-matrix relationships (Eqs. 4.1.9 and 4.1.10 in Edmonds.[27] Note mistake in Eq. 4.1.12):

$$D^l_{km}(\alpha\beta\gamma) = e^{ik\alpha}d^l_{km}(\beta)e^{im\gamma} \qquad \text{(B1a)}$$

and (Eq. 4.2.7 in Edmonds):

$$D^l_{m'm}(\alpha\beta\gamma)^* = (-1)^{m'-m}D^l_{-m',-m}(\alpha\beta\gamma)\,. \qquad \text{(B1b)}$$

(ii) Expansion of the product of two *D* matrices in terms of single *D* matrices (Eq. 4.3.2 in Edmonds):

$$D^{l_1}_{m_1' m_1}(\hat{\Omega})D^{l_2}_{m_2' m_2}(\hat{\Omega}) = \sum_{l_3 m_3' m_3}(2l+1)\begin{pmatrix} l_1 & l_2 & l_3 \\ m_1' & m_2' & m_3' \end{pmatrix} D^{l_3}_{m_3' m_3}(\hat{\Omega})^* \times \begin{pmatrix} l_1 & l_2 & l_3 \\ m_1 & m_2 & m_3 \end{pmatrix}. \qquad \text{(B2)}$$

(iii) Relationships of 3*j* symbols (Eqs. 3.7.7, 3.7.8, and 3.7.6 in Edmonds):

$$\sum_{l_3 m_3}(2l_3+1)\begin{pmatrix} l_1 & l_2 & l_3 \\ m_1' & m_2' & m_3 \end{pmatrix}\begin{pmatrix} l_1 & l_2 & l_3 \\ m_1 & m_2 & m_3 \end{pmatrix} = \delta_K(m_1' - m_1)\delta_K(m_2' - m_2)\,, \qquad \text{(B3a)}$$

$$\sum_{m_1 m_2}\begin{pmatrix} l_1 & l_2 & l_3' \\ m_1 & m_2 & m_3' \end{pmatrix}\begin{pmatrix} l_1 & l_2 & l_3 \\ m_1 & m_2 & m_3 \end{pmatrix} = (2l_3+1)^{-1}\delta_K(l_3' - l_3)\delta_K(m_3' - m_3)\delta(l_1,l_2,l_3)\,, \qquad \text{(B3b)}$$

$$\begin{pmatrix} l_1 & l_2 & l_3 \\ m_1 & m_2 & m_3 \end{pmatrix} = (-1)^{l_1+l_2+l_3}\begin{pmatrix} l_1 & l_2 & l_3 \\ -m_1 & -m_2 & -m_3 \end{pmatrix}, \qquad \text{(B3c)}$$

where $\delta(l_1,l_2,l_3) = 1$ if $|l_1 - l_2| \leqslant l_3 \leqslant l_1 + l_2$, and is zero otherwise.

(iv) Spherical harmonics: (a) Relationship to *D* matrices (Eq. 4.1.25 in Edmonds):

$$D^l_{m0}(\alpha\beta\gamma) = (-1)^m\left(\frac{4\pi}{2l+1}\right)^{1/2}Y_{lm}(\beta\alpha)\,, \qquad \text{(B4a)}$$

$$D^l_{0m}(\alpha\beta\gamma) = \left(\frac{4\pi}{2l+1}\right)^{1/2}Y_{lm}(\beta\gamma)\,. \qquad \text{(B4b)}$$

(b) Orthogonality relationships (Eqs. 2.5.4 and 4.6.6 in Edmonds):

$$\int d\hat{\Omega}\,Y^*_{l'm'}(\hat{\Omega})Y_{lm}(\hat{\Omega}) = \delta_K(l'-l)\delta_K(m'-m)\,, \qquad \text{(B5a)}$$

$$\sum_m Y^*_{lM}(\hat{\Omega})Y_{lm}(\hat{\Omega}') = \frac{(2l+1)}{4\pi}P_l[\cos(\hat{\Omega},\hat{\Omega}')]\,. \qquad \text{(B5b)}$$

[1] F. M. Penning, Naturwissenschaften XV, 818 (1927).

[2] M. B. McElroy, Planet. Space Sci. 13, 403 (1965).

[3] C. K. Rhodes, IEEE J. Quantum Elecron. 10, 153 (1974).

[4] H. Nakamura, J. Phys. Soc. Jpn. 26, 1473 (1969).

[5] H. Nakamura, J. Phys. Soc. Jpn. 31, 574 (1971).

[6] F. Koike and H. Nakamura, J. Phys. Soc. Jpn. 33, 1426 (1972).

[7] M. Mori, T. Watanabe, and K. Katsuura, J. Phys. Soc. Jpn. 19, 380 (1964).

[8] M. Mori and H. Fujita, J. Phys. Soc. Jpn. 20, 432 (1965).

[9] M. Mori, J. Phys. Soc. Jpn. 21, 979 (1966).

[10] U. Fano, Phys. Rev. 124, 1866 (1961).

[11] M. Mori, J. Phys. Soc. Jpn. 26, 773 (1969).

[12] H. Nakamura, J. Phys. Soc. Jpn. 24, 1353 (1968).

[13] H. Nakamura, J. Phys. Soc. Jpn. 25, 519 (1968).

[14] H. Nakamura, J. Phys. Soc. Jpn. 26, 614 (1969).

[15] H. Feshbach, Ann. Phys. (N.Y.) 19, 287 (1962).

[16] R. H. Lemmer, Rep. Prog. Phys. 29, 131 (1966).

[17] T. F. O'Malley, Phys. Rev. 150, 14 (1966); 156, 230 (1967).

[18] C. Bottcher, Proc. R. Soc. A 340, 301 (1974).

[19] W. H. Miller, Chem. Phys. Lett. 4, 627 (1970).

[20] R. G. Newton, *Scattering Theory of Waves and Particles* (McGraw-Hill, New York, 1966).

[21] N. F. Mott and H. S. W. Massey, *The Theory of Atomic Collisions* (Oxford U.P., New York, 1965).

[22] L. I. Schiff, *Quantum Mechanics* (McGraw-Hill, New York, 1968).

[23] W. H. Miller, H. F. Schaefer, III, and C. A. Slocomb, J. Chem. Phys. 56, 1347 (1972).

[24] H. Hotop and A. Niehaus, Z. Phys. 238, 452 (1970).

[25] K. L. Bell, J. Phys. B 3, 1308 (1970).

[26] G. W. King, *Spectroscopy and Molecular Structure* (Holt, Rinehart, and Winston, New York, 1964).

[27] A. R. Edmonds, *Angular Momentum in Quantum Mechanics* (Princeton U.P., Princeton, N.J., 1960).

[28] A. M. Arthurs and A. Dalgarno, Proc. R. Soc. Lond. 256, 540 (1960).

[29] E. S. Chang and U. Fano, Phys. Rev. A 6, 173 (1972).

[30] W. W. Robertson, J. Chem. Phys. 44, 2456 (1966).

[31] A. L. Schmeltekopf, F. C. Fehsenfeld, and G. I. Gilman, Planet. Space Sci. 15, 401 (1967).

[32] H. Fujii, H. Nakamura, and M. Mori, J. Phys. Soc. Jpn. 29, 1030 (1970).

[33] A. P. Hickman, A. D. Isaacson, and W. H. Miller, J. Chem. Phys. 66, 1483 (1977).

[34] A. P. Hickman, Ph.D. thesis (Rice University, 1973) (unpublished).

[35] A. S. Davydov, *Quantum Mechanics* (Addison-Wesley, Reading, Mass., 1965).

[36] J. C. Y. Chen and J. L. Peacher, Phys. Rev. 163, 103 (1967).

[37] R. J. Bieniek, J. Phys. B 7, L266 (1974).

[38] R. J. Bieniek, Phys. Rev. A 15, 1513 (1977).

[39] A. C. Allison, Ph.D. thesis (Glasgow University, 1967) (unpublished).

[40] A. C. Allison, J. Comput. Phys. 6, 378 (1970).

[41] A. C. Allison, Comput. Phys. Commun. 3, 173 (1972).

[42] K. Smith, *The Calculation of Atomic Collision Processes* (Wiley, New York, 1971).

[43] P. G. Burke and M. J. Seaton, in *Methods of Computational Physics*, edited by B. Alder (Academic, New-York, 1971), Vol. 10.

[44] A. P. Hickman and H. Morgner, J. Phys. B 9, 1765 (1976).

[45] W. H. Miller and H. F. Schaefer, III, J. Chem. Phys. 53, 1421 (1970).

[46] J. D. Stuart and F. A. Matsen, J. Chem. Phys. 41, 1646 (1964).

[47] L. Wolniewicz, J. Chem. Phys. 43, 1087 (1965).

[48] H. H. Michels, J. Chem. Phys. 44, 3834 (1966).

[49] A. Dalgarno and A. E. Kingston, Proc. Phys. Soc. Lond. 73, 455 (1959).

[50] W. H. Miller, J. Chem. Phys. 52, 3563 (1970).

[51] A. P. Hickman (private communication).

[52] J. S. Cohen and N. F. Lane, J. Phys. B 6, L113 (1973).

[53] H. Hotop, E. Illenberger, H. Morgner, and A. Niehaus, Chem. Phys. Lett. 10, 493 (1971).

[54] H. Morgner, Diplom. thesis (Universität Freiburg, 1971) (unpublished).

[55] E. W. McDaniel, V. Cermak, A. Dalgarno, and E. E. Ferguson, *Ion-Molecule Reactions* (Wiley, New York, 1970).

[56] H. Morgner, Doktorarbeit (Universität Freiburg, 1976) (unpublished).

[57] H. Hotop, Radiat. Res. 49, 367 (1974).

[58] R. J. Bieniek and A. Dalgarno, Astrophys. J. (to be published).

[59] P. H. Morse and H. Feshbach, *Methods of Theoretical Physics* (McGraw-Hill, New York, 1953).

[60] R. A. Buckingham, in *Quantum Theory: I. Elements*, edited by D. R. Bates (Academic, New York, 1961).